Title

A new quorum-sensing system (TprA/PhrA) for Streptococcus pneumoniaeD39 that regulates a lantibiotic biosynthesis gene cluster

Journal

Molecular Microbiology, 97(2)

ISSN

0950-382X

Authors

Hoover, SE
Perez, AJ
Tsui, HCT
et al.

Publication Date

2015-07-01

DOI

10.1111/mmi.13029

Peer reviewed

A new quorum sensing system (TprA/PhrA) for *Streptococcus pneumoniae* D39 that regulates a lantibiotic biosynthesis gene cluster

Sharon E. Hoover[1], Amilcar J. Perez[1], Ho-Ching T. Tsui[2], Dhriti Sinha[2], David L. Smiley[3], Richard D. DiMarchi[3], Malcolm E. Winkler[2], and Beth A. Lazazzera[1]

[1]Department of Microbiology, Immunology and Molecular Genetics, University of California, Los Angeles, 609 Charles E. Young Dr. East, 1602 Molecular Science Building, Los Angeles, California 90095
[2]Department of Biology, Indiana University Bloomington, Jordan Hall; 1001 East Third Street; Bloomington, Indiana 47405
[3]Department of Chemistry, Indiana University Bloomington, 800 E. Kirkwood Avenue, Bloomington, Indiana 47405

Corresponding Author:
Beth A. Lazazzera
Department of Microbiology, Immunology, and Molecular Genetics
609 Charles E. Young Dr. East
1602 Molecular Science Building
University of California, Los Angeles
Los Angeles, CA 90095

(310) 794-4804 (voice)
(310) 206-5231 (fax)
BethL@microbio.ucla.edu

Running Title: Phr-peptide signaling by *S. pneumoniae*
Keywords: Quorum sensing, Phr peptides, Lantibiotics, *Pneumococcus*

ABSTRACT

The Phr peptides of *Bacillus* species mediate quorum sensing, but their identification and function in other species of bacteria has not been determined. We have identified a Phr peptide quorum sensing system (TprA/PhrA) that controls the expression of a lantibiotic gene cluster in the Gram-positive human pathogen, *Streptococcus pneumoniae*. Lantibiotics are highly modified peptides that are part of the bacteriocin family of antimicrobial peptides. We have characterized the basic mechanism for a Phr peptide signaling system in *S. pneumoniae* and found that it induces expression of the lantibiotic genes when pneumococcal cells are at high density in the presence of galactose, a main sugar of the human nasopharynx, a highly competitive microbial environment. Activity of the Phr peptide system is not seen when pneumococcal cells are grown with glucose, the preferred carbon source and the most prevalent sugar encountered by *S. pneumoniae* during invasive disease. Thus, the lantibiotic genes are expressed under the control of both cell density signals via the Phr peptide system and nutritional signals from the carbon source present, suggesting that quorum sensing and the lantibiotic machinery may help pneumococcal cells compete for space and resources during colonization of the nasopharynx.

INTRODUCTION

Quorum sensing is carried out by small secreted molecules that diffuse through the environment, eliciting responses in proximal cells when the signaling molecules reach a critical threshold concentration (Keller & Surette, 2006, Waters & Bassler, 2005). In Gram-positive bacteria, quorum sensing often relies on recognition of small secreted peptides that signal through two-component regulatory systems (Rutherford & Bassler, 2012, Pottathil & Lazazzera, 2003, Lyon & Novick, 2004). An alternative group of quorum sensing peptides are those that signal to cells by interacting with an oligopeptide transporter and then a cytoplasmic receptor protein, which is either a member of the RNPP or the Rgg family of proteins (Rocha-Estrada *et al.*, 2010, Dunny, 2007, Jimenez & Federle, 2014, Fleuchot *et al.*, 2011, Pottathil & Lazazzera, 2003). The Phr family of signaling peptides of Bacilli belongs to the latter group, and these peptides regulate a number of important processes such as sporulation, development of genetic competence, virulence gene expression, biofilm formation, and excision and transfer of mobile genetic elements (Rocha-Estrada *et al.*, 2010, Slamti & Lereclus, 2002, Lazazzera *et al.*, 1997, Auchtung *et al.*, 2005, Bongiorni *et al.*, 2005, Perego & Hoch, 1996). However, the role that the Phr signaling peptides play outside of the Gram-positive endospore forming bacterial species has not yet been established.

The Phr family of quorum sensing peptide of Bacilli are secreted through the Sec-dependent export pathway and processed from a small precursor protein to a mature, 5-7 residue, polar peptide (Mirouze *et al.*, 2011, Aceves-Diez *et al.*, 2007, Ogura *et al.*, 2003, Perego, 1997, Solomon *et al.*, 1996, Bongiorni *et al.*, 2006). These peptides are encoded by genes typically found immediately adjacent to genes encoding their cytoplasmic target proteins, forming a quorum-sensing cassette (Pottathil & Lazazzera, 2003, Rocha-Estrada *et al.*, 2010). A classic example of the Phr peptides is **c**ompetence and **s**porulation **f**actor (CSF) of *Bacillus subtilis* (Pottathil & Lazazzera, 2003). The precursor protein for CSF, PhrC, has an N-terminal signal sequence for Sec-dependent export, and the CSF pentapeptide is derived from the C-

terminus of the protein through processing by extracellular proteases (Solomon *et al.*, 1996, Lanigan-Gerdes *et al.*, 2007, Lanigan-Gerdes *et al.*, 2008). Once CSF has reached a critical concentration, it is transported into the cell by an oligopeptide permease (Opp) and interacts with at least two intracellular receptors, RapC and RapB, to inhibit their activity (Core & Perego, 2003, Lazazzera *et al.*, 1997, Perego, 1997). Both RapB and RapC control the activity of response regulators involved in the regulation of sporulation and genetic competence, respectively (Core & Perego, 2003, Ishikawa *et al.*, 2002, Parashar *et al.*, 2013). A number of Phr peptide signaling cassettes have been found in the genomes of other Gram-positive endospore forming *Bacilli* and *Clostridia* species (Perego & Brannigan, 2001, Pottathil & Lazazzera, 2003, Slamti & Lereclus, 2005, Bongiorni *et al.*, 2006, Rocha-Estrada *et al.*, 2010). Of the non-*B. subtilis* cassettes, the best studied is the PlcR/PapR cassette of *B. cereus* and *B. thuringiensis*, in which the secreted Phr signaling peptide produced by *papR* activates the transcription factor PlcR to simulate virulence gene expression (Slamti & Lereclus, 2002, Grenha *et al.*, 2013, Gohar *et al.*, 2008, Sastalla *et al.*, 2010).

Several lines of evidence suggested that Phr peptides may play a role in the physiology of *Streptococcus pneumoniae* (pneumococcus), an important Gram-positive commensal bacterium that colonizes the human nasopharynx and is a serious opportunistic pathogen, causing significant health and financial burdens worldwide (2007, O'Brien *et al.*, 2009, Huang *et al.*, 2011). Pneumococcal Opp (encoded by *amiACDEF*), the homologue to the transporter necessary for import of *phr* peptides in Bacilli, is important for colonization and virulence in this organism (Chen *et al.*, 2008, Hava & Camilli, 2002, Molzen *et al.*, 2011, Orihuela *et al.*, 2004, Song *et al.*, 2008). How Opp influences these processes is unknown, but knockout of Opp in *S. pneumoniae* has highly pleiotropic effects, influencing amino acid uptake, adherence to human epithelial cells, and development of genetic competence (Claverys *et al.*, 2000, Trombe *et al.*, 1984, Trombe *et al.*, 1979, Alloing *et al.*, 1996, Cundell *et al.*, 1995). Additionally, Opp is upregulated in pneumococcal cells exposed to human lung epithelial cells (Song *et al.*, 2008).

As Opp plays such a central role in the physiology of *S. pneumoniae* and is essential for Phr peptide uptake in Bacilli, we hypothesized that Phr-type peptides could play a role in *S. pneumoniae* colonization or virulence.

Here we report the identification of genes involved in Phr-peptide signaling from *S. pneumoniae*. One of the Phr-peptide signaling systems, termed TprA/PhrA, is highly conserved amongst different pneumococcal serotype strains. Analysis of TprA/PhrA in *S. pneumoniae* serotype 2 strain D39 revealed that this system mediates quorum sensing and is active in media containing galactose, one of the main carbon sources encountered by pneumococcal cells during colonization of the nasopharynx. Additionally, we determined that the system controls expression of a lantibiotic biosynthesis gene cluster with the potential to produce antimicrobial peptides that may be important for competitive fitness during nasopharynx colonization.

RESULTS

In silico identification of a conserved *phr* peptide quorum sensing cassette in *S. pneumoniae*

To identify Phr peptide sensing systems in different species of *Streptococcus*, we blasted sequenced Streptococcal genomes for gene encoding proteins with similarities to the PlcR/Rap regulatory proteins of Bacilli. The region neighboring these genes was then searched for adjacent small open reading frames with the features of Phr peptides, encoding 30 to 100 residue peptide with an N-terminal signal sequence for export and a polar C-terminal region (see *Supplemental Information* for details). Using this method, we identified 53 potential Phr peptide-signaling cassettes in sequenced Streptococcal genomes (see Tables S1-3 for the complete list). In all of the cassettes identified, only homologues to PlcR from the *B. cereus* group were identified, and no homologues to the Rap proteins of *B. subtilis* were found. These PlcR-like proteins were also suggested previously to be putative Rgg transcription factors (Fleuchot *et al.*, 2011). However, these proteins lacked the adjacent gene for a small hydrophobic peptide (SHP) that is typically associated with Rgg proteins. Instead, we determined that these proteins were adjacent to small genes that have the features of Phr-type peptides (an N-terminal secretion signal and C-terminal polar region). To further determine if these cassettes could be best described as orthologs of the PlcR/PapR system of Bacilli, the secondary and tertiary structure predictions for one cassette from *S. pneumoniae* were determined using Phyre^2 (Kelley & Sternberg, 2009). The protein structure that most closely resembled the predict structure of the protein from *S. pneumoniae* was PlcR of *B. thuringiensis* (Table S4 and Figure S1). Additionally, pairwise Blast analysis revealed that these *S. pneumoniae* proteins were more similar to PlcR of *B. cereus* (E-value of $2e^{-12}$) than Rgg2 of *Streptococcus pyogenes* (E-value of $3e^{-05}$). Thus, these gene cassettes of *S. pneumoniae* appear to be orthologs of PlcR/PapR system.

PlcR orthologs were found in several Streptococcal species; however, in *S. pneumoniae* strains, the orthologs were mainly encoded adjacent to a *phr* gene (Tables S1-3). Three distinct Phr peptide-signaling cassettes were found in *S. pneumoniae* strains. Each of these cassettes has a gene for a secreted Phr peptide and a gene for a transcription factor, the PlcR ortholog, which we refer to as *tpr*, for **t**ranscription factor regulated by a **P**h**r** peptide. The first cassette (TprA/PhrA; Table S1) is conserved across 60% of sequenced pneumococcal genomes. The two other peptide systems (TprB/PhrB; Table S2 and TprC/PhrC; Table S3) are present in islands of horizontally transferred genes, including pathogenicity island 1 (PI1) and region of diversity 2 (RD2) both in TIGR4 (Blomberg *et al.*, 2009, Brown *et al.*, 2004, Obert *et al.*, 2006).

The *tprA*/*phrA* cassette of *S. pneumoniae* differs from the typical Phr-signaling cassettes. The *tprA* and *phrA* genes are oriented in opposite directions, as compared to all known Phr-signaling cassettes that have the genes oriented in the same direction (Pottathil & Lazazzera, 2003, Pomerantsev *et al.*, 2009). Interestingly, this is similar to the arrangement of the some of the Rgg/SHP peptide signaling cassettes (Chang *et al.*, 2011, Fleuchot *et al.*, 2011). Additionally, *phrA* encodes a 56-residue peptide, which is only surpassed in length by the 57-residue PhrH of *B. subtilis* and is longer than the other characterized Phr peptides of 38 to 48 residues (Slamti & Lereclus, 2002, Pottathil & Lazazzera, 2003, Mirouze *et al.*, 2011). These differences are indicative of the distinct evolutionary trajectory of this *S. pneumoniae* Phr-signaling cassette.

TprA is an inhibitor of *phrA* expression

To begin to understand the role of the TprA/PhrA cassette in *S. pneumoniae*, we constructed mutant strains that contained deletions of *tprA* or *phrA*. These deletion strains showed no significant deviation from wild-type during growth *in vitro* or virulence in a murine model for invasive disease, indicating that the deletion mutations do not alter the overall physiology of the bacteria (Figure S2). Many quorum sensing regulatory circuits, including those

regulated by Phr peptides, contain positive feedback loops to rapidly increase expression of the genes that produce the signaling molecules (Lazazzera *et al.*, 1999, Lereclus *et al.*, 1996, Kleerebezem *et al.*, 1997). To assess the activity of the TprA/PhrA system and whether *phrA* was regulated by the system, we constructed a *lacZ* transcriptional fusion to the promoter of *phrA* by fusing the intergenic region between *tprA* and *phrA* to *lacZ* and integrating this construct in single copy on the *S. pneumoniae* chromosome at *bgaA.* The gene construct results in the disruption of *bgaA,* which is the endogenous gene for ß-galactosidase (Halfmann *et al.*, 2007). During exponential growth in rich media, the levels of *phrA-lacZ* were low in the wild-type strain background are not statistically different from the levels in the Δ*phrA* mutant (Figure 1A), indicating that the TprA/PhrA system was not active under these growth conditions. In the Δ*tprA* strain background, *phrA* expression was elevated 34-fold relative to the wild-type strain (Figure 1A). The increased expression of *phrA* was due to the absence of TprA as *phrA-lacZ* levels dropped back to wild-type levels in the complemented strain (i.e. Δ*tprA* strain background with *tprA* at an ectopic locus) (Figure 1A). The same pattern of expression was seen when *phrA* expression levels were monitored directly using qRT-PCR in exponentially growing cells (Figure 1B). These data indicate that TprA serves as an inhibitor of PhrA expression and that the TprA/PhrA system was not active during growth in rich media.

PhrA can induce expression of the TprA regulon by antagonizing TprA activity

Next, we tested whether PhrA encodes a signaling peptide that can influence expression of the TprA-regulated genes. If PhrA were a co-inhibitor of the TprA regulon, an increase in *phrA-lacZ* expression would be expected in the Δ*phrA* strain background, which was not observed (Figure 1A). Alternatively, PhrA could serve as an antagonist to TprA activity, and if so, we would expect to see an increase in *phrA-lacZ* in response to PhrA. To that end, full-length *phrA* was placed under the control of a fucose-inducible promoter (P_{fcsK}), and this construct was integrated as a single copy in a strain that contained *phrA-lacZ*. We monitored

196 the levels of *phrA-lacZ* in the presence and absence of fucose and found that *phrA-lacZ* levels
197 were indeed increased in a statistically significant manner when PhrA was overexpressed
198 (Figure 2A), indicating that PhrA can activate expression of the TprA regulon and participate in
199 autoregulation.

200 Based on the work with Phr peptides in Bacilli (Slamti & Lereclus, 2002, Bouillaut *et al.*,
201 2008, Pottathil & Lazazzera, 2003), we predicted that the active PhrA signaling peptide would
202 be a small peptide derived from the C-terminus of the PhrA precursor protein. To see if such a
203 peptide was capable of activating the TprA/PhrA system, we treated cells containing the *phrA-*
204 *lacZ* reporter with a synthetic peptide corresponding to last 10 residues of PhrA. Expression of
205 *phrA* was approximately 15-fold higher in the presence of this synthetic peptide compared to the
206 levels obtained by addition of the peptide-resuspension buffer (Figure 2B-C). A similar 45-fold
207 increase in *phrA* expression was measured by qRT-PCR of wild-type cells treated with the 10-
208 residue peptide (Figure S3). To test whether the PhrA peptide acts through TprA, we examined
209 levels of the *phrA-lacZ* reporter in a Δ*tprA* background. In the presence and absence of the 10-
210 residue synthetic peptide, the levels of *phrA* expression were high in the absence of TprA
211 (Figure 2C). Taken together, these data show that PhrA can induce expression of TprA-
212 regulated genes, ostensibly by antagonizing the inhibitory activity of TprA.
213
214 **Identification of the minimal peptide form of the PhrA signaling peptide**

215 To begin to elucidate the nature of the mature PhrA signaling peptide, we took two
216 complementary approaches. First, we overexpressed PhrA proteins that lacked various portions
217 of the C-terminus. If all or part of the mature peptide were located in the deleted portions of
218 *phrA*, we would not observe induction of *phrA-lacZ*. Constructs of *phrA*, under the control of
219 P_{fcsK}, were created that lacked the last 15, 10, 5 or 1 residues of PhrA (PhrAΔ42-56, PhrAΔ47-
220 56, PhrAΔ52-56, and PhrAΔ56, respectively). Each of these truncated proteins failed to induce
221 *phrA-lacZ* (Figure 2A), consistent with idea that the mature signaling peptide is derived from the

very C-terminus of the precursor protein. Additionally, cells treated with 5 μM of synthetic peptides corresponding to the last 6, 7, or 10 residues of PhrA resulted in induction of *phrA-lacZ*. In contrast, treatment with synthetic peptides corresponding to the last 5 residues or a 6-residue internal fragment (i.e. the active 7-residue peptide but lacking the very last aspartic acid) did not induce *phrA-lacZ* (Figure 2C). These data demonstrate that the minimal peptide corresponds to the very C-terminal 6 amino acids of PhrA. Interestingly, the longer synthetic 7- and 10-residue PhrA peptides showed a greater ability to induce system activity (Figure 2C). Thus, the mature PhrA peptide produced by cells could be longer than the minimal 6-residue peptide identified in this study.

Oligopeptide permease is required for cells to respond to the synthetic PhrA peptide

Internalization of the extracellular PhrA-signaling peptide is central to the mechanism whereby the extracellular PhrA peptide signals to cells by interacting directly with TprA. Thus, we asked whether the oligopeptide permease encoded by *amiABCDE* of *S. pneumoniae* is required for responding to the PhrA-signaling peptide. To this end, expression of *phrA-lacZ* was measured in a strain that lacked *amiC* in the presence and absence of the 10-residue synthetic PhrA peptide (Figure 3). Expression of *phrA* in the strain deleted for Δ*amiC* was low and indistinguishable from isogenic wild-type cells in the absence of peptide, but failed to show induction in response to PhrA peptide treatment. A simple model for the role of Opp is to import the PhrA peptide into the cell to antagonize TprA activity. Consistent with this model, *phrA-lacZ* expression increased 21-fold in the strain lacking both *amiC* and *tprA*, as compared to the strain just lacking *amiC*, and reached a level of expression comparable to the *tprA* mutant strain (Figure 3). As expected, the strain lacking *amiC* and *tprA* was unable to respond to the 10-residue PhrA peptide. These data are in agreement with Opp functioning upstream of TprA to transport mature PhrA peptide into the cell to antagonize TprA control of gene expression.

The TprA/PhrA system is active in media containing galactose.

During growth under laboratory conditions in rich media, the TprA/PhrA signaling system is not active (Figure 1). The promoter for *phrA* is predicted to contain a CRE element for binding the carbon-catabolite repressor CcpA in *S. pneumoniae*, and expression of both *tprA* and *phrA* were found to be elevated in a Δ*ccpA* background in a microarray study (Carvalho *et al.*, 2011). These data suggest that the lack of activity for the TprA/PhrA system in the rich BHI media may be due to the inhibitory effects of glucose in the formulated Becton-Dickinson BHI media as it contains 0.2 % glucose in this media. Thus, we examined *phrA-lacZ* activity when cells were grown in chemically defined media made with either glucose or galactose as the sole carbon source (CDM-glucose or CDM-galactose, respectively) (Figure 4A). When cells containing the *phrA-lacZ* reporter were grown in CDM-glucose, the activity of the reporter remained very low throughout the growth curve (Figure 4B). However, when the same cells were grown in CDM-galactose, expression of the reporter was induced during mid-exponential growth and continued to increase throughout the growth of the culture as expected for a cell density monitoring system (Figure 4A & B). Similar results for *phrA* expression were observed by qRT-PCR (Figure S4). These data indicate that the TprA/PhrA system is active in cells grown in the presence of galactose, but not glucose.

As *phrA* expression was induced when cells were grown in CDM-galactose, we asked if a PhrA signaling peptide was produced and exported in this same media. Wild-type cells containing *phrA-lacZ* were grown in CDM-galactose to exponential phase (OD_{620} ~ 0.1) when they were collected by centrifugation and resuspended in CDM-galactose media conditioned by the growth of wild-type cells (WT CM) or Δ*phrA* mutant cells (Δ*phrA* CM). As a control, these cells were also resuspended in the original CDM-galactose growth media (untreated). Incubation of cells with WT CM resulted in a strong induction of *phrA-lacZ* after 4 hours, which was significantly higher than the induction observed with the untreated media. The inducing

activity of the conditioned media was dependent on PhrA, as Δ*phrA* CM did not induce *phrA-lacZ* (Figure 4C). These data indicate that a mature PhrA signaling peptide was present in the conditioned media from wild-type cells and that this signaling peptide is able to activate the TprA regulon when added to cells in trans.

TprA and PhrA regulate lantibiotic biosynthesis machinery

TprA is predicted to be a transcription factor, and thus, to begin to identify genes controlled by the TprA/PhrA quorum sensing system in *S. pneumoniae*, we performed whole-genome expression profiling using RNA-sequencing (RNA-seq) on cells lacking *tprA*, *phrA* or both, and on cells treated with 10-residue synthetic PhrA peptide (PhrA(10)). RNA was isolated from Δ*tprA* cells, Δ*phrA* cells, and Δ(*tprA-phrA*) cells and compared to RNA isolated from wild-type cells, and RNA isolated from wild-type cells treated with 10 μM peptide was compared to RNA isolated from cells lacking peptide treatment. Genes that were significantly differentially expressed were identified as those that had an up- or down-fold change of at least 2.0 with a false detection rate of 0.001 or lower (Table 1). Transcript levels for *tprA* (spd1745) and *phrA* (spd1746) were increased on average 10- and 28-fold, respectively, in cells lacking *tprA* or induced with PhrA(10). While *tprA* was only identified to be induced in cells treated with PhrA(10), *tprA* was not identified as differentially expressed in the strains Δ*tprA* and Δ(*tprA-phrA*) in Table 1. In strains with a deletion of *tprA* mutant, we observed an increase of transcription just 5' to the location of the *tprA* deletion (Figure S6), indicating that TprA negatively regulates its own expression. However, due to the lack of *tprA* transcription in the deleted region, the total sum of reads was below the 2-fold difference threshold through *tprA* in the Δ*tprA* or Δ(*tprA-phrA*) mutant strains compared to the wild-type strain. Thus, these data revealed *tprA* and *phrA* are transcribed divergently and autoregulate their own production.

Besides *phrA* and *tprA*, 22 genes were found to be differentially expressed in at least one of the mutant strains or cells treated with PhrA(10) (Table 1). Eleven of these genes flank

299 the *tprA, phrA* region and were differentially expressed to similar extents in both the PhrA(10)-
300 treated cells, as well as the Δ*tprA* single and Δ(*tprA-phrA*) double mutants (Table 1; Figure 5).
301 None of these genes was differentially expressed in the Δ*phrA* mutant, consistent with the levels
302 of *phrA* expression in wild-type cells being insufficient to activate expression of these genes.
303 Four genes, extending from spd0769 to spd0773 were all up-regulated in PhrA(10)-treated cells
304 and in the Δ(*tprA-phrA*) mutant, with the exception of spd0769 that was only induced in the
305 PhrA(10)-treated cells. Why these genes were not also induced in either the Δ*tprA* or Δ*phrA*
306 single mutant is unknown. The remaining seven genes were only regulated under one of the
307 conditions tested. While these genes controlled by one or two of the conditions tested are
308 potentially interesting, we choose to focus on the genes, spd1744 to spd1756, consistently
309 identified as differentially expressed under conditions of PhrA(10) treatment or loss of *tprA* (i.e.
310 the single Δ*tprA* or double Δ(*tprA-phrA*) mutant).
311 Of the thirteen genes extending from spd1744 to spd1756, at least nine of these genes
312 (spd1747 to spd1755) are predicted to be involved in synthesis of or immunity to a lantibiotic
313 peptide (Figure 5, Table 1). All of the genes in this region were upregulated in strains lacking
314 *tprA* at least 3-fold and as much as 50-fold over the levels found in the wild-type strain, and
315 were induced to a slightly lesser extent in the presence of the PhrA peptide. Four promoters are
316 predicted in this region from RNA-seq data of the wild-type strain by comparing expression
317 levels of neighboring genes (data not shown) (Figure 5). One of these predicted promoters is
318 upstream of spd1744, a gene of unknown function. A second promoter is located upstream of
319 *tprA*, which is predicted to be in a single gene operon, and this promoter most likely contributes
320 to its autoregulation. A third promoter is in located upstream of *phrA*, which is predicted to be in
321 an operon with spd1747 and spd1748, which encode lantipeptide precursor proteins. The last
322 promoter is located upstream of spd1754, which appears to be in an operon with spd1755 and
323 possibly spd1756, and encodes a putative lantipeptide transporter, an immunity protein, and a
324 protein of unknown function, respectively. The genes extending from spd1749 to spd1753,

which encode putative lantipeptide modifying enzymes, were expressed at levels that were below the threshold for promoter prediction in the wild-type strain. However, the DOOR database for predicted operons (Mao *et al.*, 2009) indicates that potential promoters are upstream of spd1749 and spd1750. We were unable to identify any conserved inverted repeats in the putative promoter regions (see Supplemental Material and Methods). Thus, the binding-site for TprA is unknown, and future research is necessary to identify its binding site.

To validate the RNA-seq data, qRT-PCR was performed to confirm the regulation by the TprA on several of the key lantibiotic biosynthesis genes: the lantibiotic precursor peptides, spd1747 and spd1748 (these genes were probed together in the qRT-PCR analysis due to their small size), the bifunctional modification enzyme encoding by spd1749, a second predicted lantibiotic biosynthesis enzyme encoded by spd1750, and the gene that encodes the predicted immunity protein, spd1754 (Figure 5). RNA from wild-type, Δ*tprA* and Δ*tprA*-complemented strains were isolated from mid-exponentially growing cells and subjected to qRT-PCR analysis. TprA-dependent inhibition of expression was observed for all 4 sets of genes as probe levels increased significantly in the Δ*tprA* strain compared to wild-type and dropped again to near-wild-type levels in the Δ*tprA*-complemented strain (Figure S5).

To confirm that the extracellular PhrA peptide could also activate expression of the lantibiotic machinery, we performed qRT-PCR analysis for these same 4 sets of genes on RNA isolated from mid-exponential wild-type cells that had been treated with the synthetic 10-residue PhrA peptide. Again, we observed significant upregulation of all 4 sets of genes in the cells that were treated with the synthetic peptide compared to those that had been treated with the peptide-resuspension buffer alone (Figure S5). The data from the RNA-seq analysis and subsequent validation of the regulation of several key lantibiotic genes by qRT-PCR indicate that the TprA/PhrA signaling system controls expression of the adjacent putative lantibiotic biosynthesis gene cluster.

DISCUSSION

We report here the identification and characterization of a new quorum-sensing cassette in *S. pneumoniae* D39 that belongs to the Phr family of quorum-sensing systems, which had previously only been identified in Gram-positive, endospore-forming bacteria. Through RNA-seq analysis, the PhrA peptide was found to induce genes that appear to process and provide immunity to a lantibiotic peptide. The expression of *phrA* and the corresponding lantibiotic genes were shown to be inhibited by the presence of glucose and to be induced in the presence of galactose. Galactose is the major sugar in the human nasopharynx (King, 2010, Yesilkaya *et al.*, 2008), consistent with a role for TprA/PhrA and the lantibiotic peptide in colonization of the host.

Lantibiotics are highly modified peptides that fall in the bacteriocin family of small antimicrobial peptides produced by many bacterial species and have been implicated in inter- and intra-species competition. These peptides are ribosomally synthesized and can have broad- or narrow-spectrum antimicrobial activity against other bacteria (Cotter *et al.*, 2005, Cotter *et al.*, 2013). *S. pneumoniae* is already known to produce the Blp bacteriocin that is responsible for mediating intra-species competition amongst a few *S. pneumoniae* clinical isolates during host nasopharynx colonization (Dawid *et al.*, 2007). Antibacterial activity of the lantibiotic system controlled by pneumococcal TprA/PhrA was suggested by experiments in a heterologous system. When the two lantibiotic-precursor peptides from *S. pneumoniae* were produced and modified using the nisin machinery from *Lactococcus lactus*, the peptides exhibited antimicrobial activity against *Micrococcus flavus*, an organism that colonizes humans (Majchrzykiewicz *et al.*, 2010). Given the necessity for inter- as well as intra-species competition during nasopharynx colonization, lantibiotic biosynthesis machinery may represent a mechanism for interspecies competition in the nasopharynx. At this time, we cannot rule out other possible functions for the lantibiotic gene cluster, spd1744-spd1756. Lantipeptides produced by *Streptomyces* spp. have surfactant activity and are used to reduce surface tension for aerial hyphae formation (Willey &

van der Donk, 2007, Kodani *et al.*, 2004, Kodani *et al.*, 2005). Surfactants have also been implicated in biofilm formation in a number of bacterial species (Otto, 2013, Raaijmakers *et al.*, 2010), and biofilm formation has recently been implicated in colonization of the nasopharynx by *S. pneumoniae* (Munoz-Elias *et al.*, 2008, Marks *et al.*, 2012a, Marks *et al.*, 2012b). Experiments are currently underway to identify the biological role for this lantibiotic biosynthesis gene cluster.

A model for the mechanism by which TprA/PhrA induce the lantibiotic biosynthesis gene cluster is presented in Figure 6. The PhrA signaling peptide is derived from a precursor protein that is predicted to be exported through the Sec pathway and processed outside the cell by proteases to release the mature peptide, whose minimal form is the C-terminal 6 residues of the PhrA-precursor protein. Once the PhrA peptide has reached a sufficient extracellular concentration, it interacts with Opp whereby it is predicted to be brought into the cytoplasm and antagonize the inhibitory activity of TprA to induce expression of the peptide-encoding gene itself, *tprA,* and the lantibiotic biosynthesis gene cluster. At this time, we cannot rule out that TprA and/or PhrA may control more genes than those identified through the growth condition used in this study. Consistent with this possibility, the *tprA*/*phrA* genes are highly conserved in other *S. pneumoniae* serotype strains, but the lantibiotic biosynthetic cluster genes are not.

We found that the TprA/PhrA system is active and capable of signaling between cells when grown in media that contains galactose, but not glucose. The differential expression of these genes in response to glucose versus galactose appears to be mediated via the canonical, carbon catabolite control mechanism of Gram-positive bacteria, in which the CcpA protein binds to CRE elements in promoters when cells are grown in the presence of glucose (Sonenshein, 2007). The promoter for *phrA* is predicted to contain a CRE-binding site for the pneumococcal CcpA (Carvalho *et al.*, 2011). In this context, it is interesting to note that genes involved in sugar metabolism, including PTS system components (e.g. spd0771-0773), were differentially expressed in PhrA peptide treated cells, but the significance of this regulation is unknown as a

402 Δ*tprA* mutation did not significantly induce the expression of these same genes. The expression
403 levels for *tprA*, *phrA*, and many members of the putative lantibiotic biosynthesis gene cluster
404 were upregulated in a strain that lacked CcpA compared to a wild-type strain when the cells
405 were grown in the presence of glucose (Carvalho *et al.*, 2011). Expression of the lantibiotic
406 gene cluster has also been shown to be inhibited by the CiaRH two-component regulatory
407 system (Mascher *et al.*, 2003); although at this time there is no data to suggest that CiaRH
408 mediates catabolite control of this gene cluster. These data indicate that the production of the
409 lantibiotic biosynthesis machinery is part of the carbon-catabolite response of *S. pneumoniae*,
410 and is the first example, to our knowledge, of a lantibiotic incorporated into the carbon-catabolite
411 regulon.
412 The differential regulation of the TprA-regulon based on available carbon source is
413 interesting when placed in the context of where the pneumococcal cells may encounter glucose
414 or galactose in the human host. Glucose is the preferred carbon source for pneumococcal cells
415 and found in large amounts in the bloodstream and respiratory tract of the host, areas which are
416 normally low in bacterial counts (Philips *et al.*, 2003). Galactose, in contrast, is one of the main
417 carbon sources that pneumococcal cells encounter in the nasopharynx during colonization
418 where they need to compete with other strains of *S. pneumoniae* and other bacterial species for
419 space and resources (King, 2010, Yesilkaya *et al.*, 2008). These data are consistent with recent
420 Tn-Seq analysis that showed that transposon insertions in *tprA* or in some of the genes of the
421 lantibiotic biosynthesis operon significantly reduced the fitness of *S. pneumoniae* serotype 4
422 strain TIGR4 for nasopharynx colonization in a murine model (van Opijnen & Camilli, 2012).
423 Thus, the TprA/PhrA system and its controlled lantibiotic genes are important for *S. pneumoniae*
424 to colonize the nasopharynx.
425 Consistent with a role for the TprA/PhrA system in colonization is the finding that these
426 genes and the lantibiotic gene cluster are not required for invasive disease. The Tn-Seq study
427 previously mentioned did not detect a role for the TprA/PhrA system in murine model of invasive

428 disease (van Opijnen & Camilli, 2012). Likewise, we found that deletion of either *tprA* or *phrA*
429 has no overt effect on a murine pneumonia model (Fig S2). Consistent with the lack of a role for
430 antimicrobial activity during invasive disease by *S. pneumoniae*, others have observed that Blp
431 bacteriocin production is down regulated in mice during invasive pneumococcal disease
432 compared to growth *in vitro* (Orihuela *et al.*, 2004).
433 In order to effectively combat pneumococcal disease, a detailed understanding of the
434 mechanisms that mediate *S. pneumoniae* inter- and intra-species interactions is essential, yet
435 little is known about the genetic and molecular basis for these exchanges. The TprA/PhrA
436 quorum sensing system control of lantibiotic production may be one method employed by
437 pneumococcal cells to ensure competitive fitness during colonization of the human host. Further
438 characterization of this system will increase our understanding of pneumococcal colonization
439 and possibly lead to new targets for antimicrobial therapies.
440

EXPERIMENTAL PROCEDURES

Bacterial strains and growth conditions

Strains used in this study are derivatives of encapsulated, virulent serotype 2 strain D39 (Table S5). Details of mutant strains and constructs generated for this work are found in the *Supplemental Information.* Pneumococcal strains were grown at 37°C with 5% CO_2, either on Trypticase Soy Agar II plates (modified; Becton-Dickinson) with 5% (vol/vol) defibrinated sheep blood (TSAII-BA), in Becton-Dickinson brain heart infusion (BHI) broth, or in chemically defined media (Kazmierczak *et al.*, 2009) with 1% glucose (wt/vol) (CDM-glucose) or 1% (wt/vol) galactose (CDM-galactose) as the sole carbon source. Liquid cultures were grown statically and monitored by optical density at 620 nm (OD_{620}) using a Spectronic 20 or a Teysche 100 spectrophotometer. Starter cultures of pneumococcal strains were inoculated from frozen glycerol stocks into BHI broth, serial diluted in the same media, and propagated for 8-16 hours. For growth in BHI broth, starter cultures still in exponential phase (OD_{620} of 0.1 to 0.4) were diluted to an OD_{620} of 0.002 to 0.005 to start final cultures. For the overexpression of PhrA, the final cultures were grown in BHI broth that contained 1% (wt/vol) L-fucose. For growth in CDM-glucose and CDM-galactose, the cells of starter cultures were collected by microcentrifugation at 3000 x *g* for 10 minutes at room temperature. The cells were washed, resuspended, and diluted in CDM-glucose or CDM-galactose to an OD_{620} of 0.001 to 0.005 to start final cultures. For antibiotic selections, TSAII-BA plates or BHI broth cultures were supplemented with 0.3 µg/ml erythromycin, 250 µg/ml kanamycin, 250 µg/ml streptomycin, or 0.25 µg/ml tetracycline.

β-galactosidase assays

β-galactosidase specific activity ([A_{420} per min per ml of culture per OD_{620}] x 1,000) was determined essentially as described previously (Hoover *et al.*, 2010), except that cell lysis was achieved by incubating cells in lysis buffer containing TritonX-100 to induce autolysis as in (Zahner & Hakenbeck, 2000). Conditioned media for use in these assays was produced by

culturing *S. pneumoniae* strains in CDM-galactose to a high cell density (OD_{620} of > 1.0), removing the cells by centrifugation at 7000 x *g* for 5 minutes at room temperature, and sterilization of the supernatant through 0.22 µm filters. For the assays in conditioned media, 30 mL cultures of exponentially growing cells (OD_{620} of ~0.3) were divided into 6 mL aliquots, the cells collected by centrifugation at 7000 x *g* at room temperature for 5 minutes, and the cell pellets resuspended in the appropriate conditioned media. Samples were removed at the indicated time for β-galactosidase assays. Reporter construct expression was compared as indicated by performing unpaired two-tailed t tests.

RNA extraction

To isolate RNA for qRT-PCR analysis, starter cultures were used to inoculate 6 ml cultures of BHI broth or CDM-galactose. RNA was extracted from 4 mL of exponentially growing cultures (OD_{620} of ~0.2) using a hot-lysis, acid-phenol extraction followed by purification using an RNeasy minikit (Qiagen) and on-column DNase I treatment as described in (Barendt *et al.*, 2009, Kazmierczak *et al.*, 2009, Ramos-Montanez *et al.*, 2008). 5 µg of total RNA was further digested with DNase using a DNA-free kit (Ambion) prior to qRT-PCR analysis. To isolate RNA for RNA-sequencing analysis, starter cultures were used to inoculate 30 ml cultures of BHI broth in 50 mL conical tubes. RNA was extracted from 23 mL of exponentially growing culture (OD_{620} of ~0.15) using the FastRNA Pro Blue Kit (MP Bio) according to the manufacturer's guidelines. Briefly, cells were isolated by centrifugation at 14,500 x *g* for 5 minutes at 4°C. The cells were resuspended in 1 ml RNA*pro* (MP Bio) and processed twice in the Fast Prep Instrument (MP Bio) for 40 seconds at a setting of 6.0. Chloroform and 100% ethanol were used to extract and precipitate the RNA from the resulting lysate and the miRNeasy minikit (Qiagen) and on-column DNase I treatments were used to purify the RNA as above. The amount and purity of all RNA samples isolated were assessed by NanoDrop spectroscopy (Thermo Fisher). RNA integrity was assessed using the Agilent 2100 BioAnalyzer (Aligent Technologies).

qRT-PCR

qRT-PCR was performed using a two-step protocol as in (Ramos-Montanez *et al.*, 2008, Kazmierczak *et al.*, 2009). Specifically, cDNA was synthesized from 100 ng of total RNA and random primers using the qScript Flex cDNA Kit (Quanta BioSciences). RT-PCR was performed using the Brilliant SYBR Green qPCR Master Mix (Stratagene), the Brilliant III Ultra-Fast SYBR Green qPCR Master Mix (Agilent), or the FastStart Universal SYBR Green Master Mix (Roche) and appropriate primers (see Table S6) as in (Kazmierczak *et al.*, 2009, Ramos-Montanez *et al.*, 2008). Reactions were performed in duplicate and normalized to 16S rRNA amounts. The 16S rRNA was quantified using the same cDNA samples except that the samples were diluted 100-fold further. Data were collected on an MX3000P thermocycler (Stratagene) or on a CFX96 thermocycler (Bio Rad) and analyzed with the SYBR Green (with dissociation curve) program associated with each machine. Four dilutions of cDNA from *S. pneumoniae* strains wild-type for *tprA* and *phrA* (either IU1781 or Spn049) were used to generate standard curves for each primer set. Normalized transcript amounts were compared as indicated by performing pairwise unpaired two-tailed t tests.

Synthetic peptides

Peptides were synthesized on a modified Applied Biosystems 430A peptide synthesizer using 0.2 mmol of 4-hydroxymethyl-phenylacetamidomethyl (PAM) resin (Midwest Biotech) and subsequently purified using reverse phase HPLC (RP-HPLC). For complete details, see *Supplementary Information*. Synthetic peptides were resuspended in 10 mM Tris pH 7.4 with 50 µg/ml BSA to a concentration of 5 mM. For β-galactosidase or qRT-PCR assays, the indicated synthetic peptide (or the peptide-resuspension buffer) was added at final concentration of 5 µM to each 6 ml cell aliquot.

Library construction and RNA-sequencing

cDNA libraries were prepared from total RNA by the University of Wisconsin-Madison Biotechnology Center. The mRNA was enriched from two micrograms total RNA using RiboZeroTM rRNA Removal (Gram-positive bacteria) Kit (EpiCentre Inc.). rRNA-depleted mRNA samples were purified by ethanol precipitation and quantified by fluorometry with the Qubit® RNA assay kit (Invitrogen). Double stranded cDNA synthesis was performed following ScriptSeqTM v2 RNA-Seq Library Preparation guide (EpiCentre Inc.) in accordance with the manufacturer's standard protocol. Thirty nanograms of enriched mRNA were fragmented using divalent cations via incubation for 5 min at 85°C. The first strand of cDNA was synthesized by reverse transcription using random-sequence primers containing a tagging sequence at their 5' ends. Di-tagged cDNA was synthesized by random annealing of a terminal-Tagging Oligo (TTO) to the 3' end of the cDNA for extension of the cDNA by DNA polymerase. Di-tagged cDNA was purified using Agencourt AMPure® XP beads (Beckman Coulter) followed by PCR amplification for 15 cycles using FailsafeTM PCR enzyme and ScriptSeq Index DNA primer set (EpiCentre Inc.). This step generated the second strand of cDNA and completed the addition of Illumina adapter sequences incorporating a user-defined barcode. The amplified libraries were purified using Agencourt AMPure® XP beads. Quality and quantity were assessed using an Agilent DNA 1000 chip (Agilent) and Qubit® dsDNA HS assay kit (Invitrogen), respectively. Libraries were standardized to 2 μM. Cluster generation was performed using standard Cluster kits (v3) and Illumina Cluster Station. Single-end 100 bp sequencing was performed using standard SBS chemistry (v3) on an Illumina HiSeq2000 sequencer. Images were analyzed using the standard Illumina pipeline, version 1.8.2.

RNA-seq analysis

The raw sequencing reads were quality and adapter trimmed using Trimmomatic (Lohse *et al.*, 2012) with a minimum length of 90. The trimmed reads were mapped on the

Streptococcus pneumoniae D39 (RefSeq NC_008533) genome and D39 plasmid pDP1 sequence (RefSeq NC_005022) using bowtie2 (Langmead & Salzberg, 2012). Custom PERL scripts were used to generate read counts for the genes and 100 bp non-overlapping intergenic regions of the genome. Differential gene expression was identified using EdgeR (version 3.6.2) using default parameters (Robinson *et al.*, 2010). The false discovery rate (FDR) was calculated using Benjamini and Hochberg's algorithm (Benjamini & Hochberg, 1995) and a gene or region was defined as differentially expressed if it had an up- or down-fold change of 2.0 and their FDR was less than 0.001.

ACKNOWLEDGMENTS

We thank Reinhold Brückner for pPP2, Kyle J. Wayne for bacterial strains, and John Lisher for instruction in CDM preparation. We thank Kurt Zimmer and Doug Rusch for assistance in analysis of RNA-seq data. We thank the members of the Lazazzera laboratory, members of the Winkler laboratory, and many generous colleagues for helpful discussions.

This work was supported by NIH grant AI48616 to B.A.L. and AI095814 and AI107075 to M.E.W. and by funds from the Indiana University Bloomington METACyt Initiative, funded in part by a major grant from the Lilly Endowment (M.E.W). S.E.H. was supported by an NIH postdoctoral training grant (5T32AI007323). A.J.P. was supported by an NIH IMSD grant (R25GM055052). The authors declare that they have no conflict of interest with the research presented.

REFERENCES

(2007) Pneumococcal conjugate vaccine for childhood immunization--WHO position paper. *Wkly Epidemiol Rec* **82**: 93-104.

Aceves-Diez, A.E., R. Robles-Burgueno & M. de la Torre, (2007) SKPDT is a signaling peptide that stimulates sporulation and cry1Aa expression in Bacillus thuringiensis but not in Bacillus subtilis. *Appl Microbiol Biotechnol*.

Alloing, G., C. Granadel, D.A. Morrison & J.P. Claverys, (1996) Competence pheromone, oligopeptide permease, and induction of competence in Streptococcus pneumoniae. *Mol Microbiol* **21**: 471-478.

Auchtung, J.M., C.A. Lee, R.E. Monson, A.P. Lehman & A.D. Grossman, (2005) Regulation of a Bacillus subtilis mobile genetic element by intercellular signaling and the global DNA damage response. *Proc Natl Acad Sci U S A* **102**: 12554-12559.

Barendt, S.M., A.D. Land, L.T. Sham, W.L. Ng, H.C. Tsui, R.J. Arnold & M.E. Winkler, (2009) Influences of capsule on cell shape and chain formation of wild-type and pcsB mutants of serotype 2 Streptococcus pneumoniae. *J Bacteriol* **191**: 3024-3040.

Benjamini, Y. & Y. Hochberg, (1995) Controlling the false discovery rate: a practical and powerful approach to multiple testing. *Journal of the Royal Statistical Society. Series B (Methodological)* **57**: 289-300.

Blomberg, C., J. Dagerhamn, S. Dahlberg, S. Browall, J. Fernebro, B. Albiger, E. Morfeldt, S. Normark & B. Henriques-Normark, (2009) Pattern of accessory regions and invasive disease potential in Streptococcus pneumoniae. *J Infect Dis* **199**: 1032-1042.

Bongiorni, C., S. Ishikawa, S. Stephenson, N. Ogasawara & M. Perego, (2005) Synergistic regulation of competence development in Bacillus subtilis by two Rap-Phr systems. *J Bacteriol* **187**: 4353-4361.

Bongiorni, C., R. Stoessel, D. Shoemaker & M. Perego, (2006) Rap phosphatase of virulence plasmid pXO1 inhibits Bacillus anthracis sporulation. *J Bacteriol* **188**: 487-498.

Bouillaut, L., S. Perchat, S. Arold, S. Zorrilla, L. Slamti, C. Henry, M. Gohar, N. Declerck & D. Lereclus, (2008) Molecular basis for group-specific activation of the virulence regulator PlcR by PapR heptapeptides. *Nucleic Acids Res* **36**: 3791-3801.

Brown, J.S., S.M. Gilliland, B.G. Spratt & D.W. Holden, (2004) A locus contained within a variable region of pneumococcal pathogenicity island 1 contributes to virulence in mice. *Infect Immun* **72**: 1587-1593.

Carvalho, S.M., T.G. Kloosterman, O.P. Kuipers & A.R. Neves, (2011) CcpA ensures optimal metabolic fitness of Streptococcus pneumoniae. *PLoS One* **6**: e26707.

Chang, J.C., B. LaSarre, J.C. Jimenez, C. Aggarwal & M.J. Federle, (2011) Two group A streptococcal peptide pheromones act through opposing Rgg regulators to control biofilm development. *PLoS Pathog* **7**: e1002190.

Chen, H., Y. Ma, J. Yang, C.J. O'Brien, S.L. Lee, J.E. Mazurkiewicz, S. Haataja, J.H. Yan, G.F. Gao & J.R. Zhang, (2008) Genetic requirement for pneumococcal ear infection. *PLoS One* **3**: e2950.

Claverys, J.P., B. Grossiord & G. Alloing, (2000) Is the Ami-AliA/B oligopeptide permease of Streptococcus pneumoniae involved in sensing environmental conditions? *Res Microbiol* **151**: 457-463.

Core, L. & M. Perego, (2003) TPR-mediated interaction of RapC with ComA inhibits response regulator-DNA binding for competence development in *Bacillus subtilis*. *Mol Microbiol* **49**: 1509-1522.

Cotter, P.D., C. Hill & R.P. Ross, (2005) Bacteriocins: developing innate immunity for food. *Nat Rev Microbiol* **3**: 777-788.

Cotter, P.D., R.P. Ross & C. Hill, (2013) Bacteriocins - a viable alternative to antibiotics? *Nat Rev Microbiol* **11**: 95-105.

614 Cundell, D.R., B.J. Pearce, J. Sandros, A.M. Naughton & H.R. Masure, (1995) Peptide
615 permeases from Streptococcus pneumoniae affect adherence to eucaryotic cells. *Infect*
616 *Immun* **63**: 2493-2498.
617 Dawid, S., A.M. Roche & J.N. Weiser, (2007) The blp bacteriocins of Streptococcus
618 pneumoniae mediate intraspecies competition both in vitro and in vivo. *Infection and*
619 *immunity* **75**: 443-451.
620 Dunny, G.M., (2007) The peptide pheromone-inducible conjugation system of Enterococcus
621 faecalis plasmid pCF10: cell-cell signalling, gene transfer, complexity and evolution.
622 *Philosophical transactions of the Royal Society of London* **362**: 1185-1193.
623 Fleuchot, B., C. Gitton, A. Guillot, J. Vidic, P. Nicolas, C. Besset, L. Fontaine, P. Hols, N.
624 Leblond-Bourget, V. Monnet & R. Gardan, (2011) Rgg proteins associated with
625 internalized small hydrophobic peptides: a new quorum-sensing mechanism in
626 streptococci. *Molecular microbiology* **80**: 1102-1119.
627 Gohar, M., K. Faegri, S. Perchat, S. Ravnum, O.A. Okstad, M. Gominet, A.B. Kolsto & D.
628 Lereclus, (2008) The PlcR virulence regulon of Bacillus cereus. *PLoS One* **3**: e2793.
629 Grenha, R., L. Slamti, M. Nicaise, Y. Refes, D. Lereclus & S. Nessler, (2013) Structural basis for
630 the activation mechanism of the PlcR virulence regulator by the quorum-sensing signal
631 peptide PapR. *Proc Natl Acad Sci U S A* **110**: 1047-1052.
632 Halfmann, A., R. Hakenbeck & R. Bruckner, (2007) A new integrative reporter plasmid for
633 Streptococcus pneumoniae. *FEMS Microbiol Lett* **268**: 217-224.
634 Hava, D.L. & A. Camilli, (2002) Large-scale identification of serotype 4 Streptococcus
635 pneumoniae virulence factors. *Mol Microbiol* **45**: 1389-1406.
636 Hoover, S.E., W. Xu, W. Xiao & W.F. Burkholder, (2010) Changes in DnaA-dependent gene
637 expression contribute to the transcriptional and developmental response of Bacillus
638 subtilis to manganese limitation in Luria-Bertani medium. *J Bacteriol* **192**: 3915-3924.
639 Huang, S.S., K.M. Johnson, G.T. Ray, P. Wroe, T.A. Lieu, M.R. Moore, E.R. Zell, J.A. Linder,
640 C.G. Grijalva, J.P. Metlay & J.A. Finkelstein, (2011) Healthcare utilization and cost of
641 pneumococcal disease in the United States. *Vaccine* **29**: 3398-3412.
642 Ishikawa, S., L. Core & M. Perego, (2002) Biochemical characterization of aspartyl phosphate
643 phosphatase interaction with a phosphorylated response regulator and its inhibition by a
644 pentapeptide. *J Biol Chem* **277**: 20483-20489.
645 Jimenez, J.C. & M.J. Federle, (2014) Quorum sensing in group A Streptococcus. *Frontiers in*
646 *cellular and infection microbiology* **4**: 127.
647 Kazmierczak, K.M., K.J. Wayne, A. Rechtsteiner & M.E. Winkler, (2009) Roles of rel(Spn) in
648 stringent response, global regulation and virulence of serotype 2 Streptococcus
649 pneumoniae D39. *Mol Microbiol* **72**: 590-611.
650 Keller, L. & M.G. Surette, (2006) Communication in bacteria: an ecological and evolutionary
651 perspective. *Nat Rev Microbiol* **4**: 249-258.
652 Kelley, L.A. & M.J. Sternberg, (2009) Protein structure prediction on the Web: a case study
653 using the Phyre server. *Nat Protoc* **4**: 363-371.
654 King, S.J., (2010) Pneumococcal modification of host sugars: a major contributor to colonization
655 of the human airway? *Mol Oral Microbiol* **25**: 15-24.
656 Kleerebezem, M., L.E. Quadri, O.P. Kuipers & W.M. de Vos, (1997) Quorum sensing by peptide
657 pheromones and two-component signal-transduction systems in Gram-positive bacteria.
658 *Mol Microbiol* **24**: 895-904.
659 Kodani, S., M.E. Hudson, M.C. Durrant, M.J. Buttner, J.R. Nodwell & J.M. Willey, (2004) The
660 SapB morphogen is a lantibiotic-like peptide derived from the product of the
661 developmental gene ramS in Streptomyces coelicolor. *Proc Natl Acad Sci U S A* **101**:
662 11448-11453.

663 Kodani, S., M.A. Lodato, M.C. Durrant, F. Picart & J.M. Willey, (2005) SapT, a lanthionine-
664 containing peptide involved in aerial hyphae formation in the streptomycetes. *Mol*
665 *Microbiol* **58**: 1368-1380.
666 Langmead, B. & S.L. Salzberg, (2012) Fast gapped-read alignment with Bowtie 2. *Nat Methods*
667 **9**: 357-359.
668 Lanigan-Gerdes, S., G. Briceno, A.N. Dooley, K.F. Faull & B.A. Lazazzera, (2008) Identification
669 of residues important for cleavage of the extracellular signaling peptide CSF of Bacillus
670 subtilis from its precursor protein. *J Bacteriol* **190**: 6668-6675.
671 Lanigan-Gerdes, S., A.N. Dooley, K.F. Faull & B.A. Lazazzera, (2007) Identification of subtilisin,
672 Epr and Vpr as enzymes that produce CSF, an extracellular signalling peptide of *Bacillus*
673 *subtilis*. *Mol Microbiol* **65**: 1321-1333.
674 Lazazzera, B.A., I.G. Kurtser, R.S. McQuade & A.D. Grossman, (1999) An autoregulatory circuit
675 affecting peptide signaling in Bacillus subtilis. *J Bacteriol* **181**: 5193-5200.
676 Lazazzera, B.A., J.M. Solomon & A.D. Grossman, (1997) An exported peptide functions
677 intracellularly to contribute to cell density signaling in B. subtilis. *Cell* **89**: 917-925.
678 Lereclus, D., H. Agaisse, M. Gominet, S. Salamitou & V. Sanchis, (1996) Identification of a
679 Bacillus thuringiensis gene that positively regulates transcription of the
680 phosphatidylinositol-specific phospholipase C gene at the onset of the stationary phase.
681 *J Bacteriol* **178**: 2749-2756.
682 Lohse, M., A.M. Bolger, A. Nagel, A.R. Fernie, J.E. Lunn, M. Stitt & B. Usadel, (2012) RobiNA: a
683 user-friendly, integrated software solution for RNA-Seq-based transcriptomics. *Nucleic*
684 *Acids Res* **40**: W622-627.
685 Lyon, G.J. & R.P. Novick, (2004) Peptide signaling in Staphylococcus aureus and other Gram-
686 positive bacteria. *Peptides* **25**: 1389-1403.
687 Majchrzykiewicz, J.A., J. Lubelski, G.N. Moll, A. Kuipers, J.J. Bijlsma, O.P. Kuipers & R. Rink,
688 (2010) Production of a class II two-component lantibiotic of Streptococcus pneumoniae
689 using the class I nisin synthetic machinery and leader sequence. *Antimicrob Agents*
690 *Chemother* **54**: 1498-1505.
691 Mao, F., P. Dam, J. Chou, V. Olman & Y. Xu, (2009) DOOR: a database for prokaryotic
692 operons. *Nucleic Acids Res* **37**: D459-463.
693 Marks, L.R., G.I. Parameswaran & A.P. Hakansson, (2012a) Pneumococcal interactions with
694 epithelial cells are crucial for optimal biofilm formation and colonization in vitro and in
695 vivo. *Infect Immun* **80**: 2744-2760.
696 Marks, L.R., R.M. Reddinger & A.P. Hakansson, (2012b) High levels of genetic recombination
697 during nasopharyngeal carriage and biofilm formation in Streptococcus pneumoniae.
698 *MBio* **3**.
699 Mascher, T., D. Zahner, M. Merai, N. Balmelle, A.B. de Saizieu & R. Hakenbeck, (2003) The
700 Streptococcus pneumoniae cia regulon: CiaR target sites and transcription profile
701 analysis. *J Bacteriol* **185**: 60-70.
702 Mirouze, N., V. Parashar, M.D. Baker, D.A. Dubnau & M.B. Neiditch, (2011) An atypical Phr
703 peptide regulates the developmental switch protein RapH. *J Bacteriol* **193**: 6197-6206.
704 Molzen, T.E., P. Burghout, H.J. Bootsma, C.T. Brandt, C.E. van der Gaast-de Jongh, M.J.
705 Eleveld, M.M. Verbeek, N. Frimodt-Moller, C. Ostergaard & P.W. Hermans, (2011)
706 Genome-wide identification of Streptococcus pneumoniae genes essential for bacterial
707 replication during experimental meningitis. *Infect Immun* **79**: 288-297.
708 Munoz-Elias, E.J., J. Marcano & A. Camilli, (2008) Isolation of Streptococcus pneumoniae
709 biofilm mutants and their characterization during nasopharyngeal colonization. *Infection*
710 *and immunity* **76**: 5049-5061.
711 O'Brien, K.L., L.J. Wolfson, J.P. Watt, E. Henkle, M. Deloria-Knoll, N. McCall, E. Lee, K.
712 Mulholland, O.S. Levine & T. Cherian, (2009) Burden of disease caused by

Streptococcus pneumoniae in children younger than 5 years: global estimates. *Lancet* **374**: 893-902.
Obert, C., J. Sublett, D. Kaushal, E. Hinojosa, T. Barton, E.I. Tuomanen & C.J. Orihuela, (2006) Identification of a Candidate Streptococcus pneumoniae core genome and regions of diversity correlated with invasive pneumococcal disease. *Infect Immun* **74**: 4766-4777.
Ogura, M., K. Shimane, K. Asai, N. Ogasawara & T. Tanaka, (2003) Binding of response regulator DegU to the aprE promoter is inhibited by RapG, which is counteracted by extracellular PhrG in *Bacillus subtilis. Mol Microbiol.* **49**: 1685-1697.
Orihuela, C.J., J.N. Radin, J.E. Sublett, G. Gao, D. Kaushal & E.I. Tuomanen, (2004) Microarray analysis of pneumococcal gene expression during invasive disease. *Infection and immunity* **72**: 5582-5596.
Otto, M., (2013) Staphylococcal infections: mechanisms of biofilm maturation and detachment as critical determinants of pathogenicity. *Annual review of medicine* **64**: 175-188.
Parashar, V., P.D. Jeffrey & M.B. Neiditch, (2013) Conformational change-induced repeat domain expansion regulates Rap phosphatase quorum-sensing signal receptors. *PLoS biology* **11**: e1001512.
Perego, M., (1997) A peptide export-import control circuit modulating bacterial development regulates protein phosphatases of the phosphorelay. *Proc Natl Acad Sci USA* **94**: 8612-8617.
Perego, M. & J.A. Brannigan, (2001) Pentapeptide regulation of aspartyl-phosphate phosphatases. *Peptides* **22**: 1541-1547.
Perego, M. & J.A. Hoch, (1996) Cell-cell communication regulates the effects of protein aspartate phosphatases on the phosphorelay controlling development in *Bacillus subtilis*. *Proc Natl Acad Sci USA* **93**: 1549-1553.
Philips, B.J., J.X. Meguer, J. Redman & E.H. Baker, (2003) Factors determining the appearance of glucose in upper and lower respiratory tract secretions. *Intensive Care Med* **29**: 2204-2210.
Pomerantsev, A.P., O.M. Pomerantseva, A.S. Camp, R. Mukkamala, S. Goldman & S.H. Leppla, (2009) PapR peptide maturation: role of the NprB protease in Bacillus cereus 569 PlcR/PapR global gene regulation. *FEMS Immunol Med Microbiol* **55**: 361-377.
Pottathil, M. & B.A. Lazazzera, (2003) The extracellular Phr peptide-Rap phosphatase signaling circuit of Bacillus subtilis. *Front Biosci* **8**: d32-45.
Raaijmakers, J.M., I. De Bruijn, O. Nybroe & M. Ongena, (2010) Natural functions of lipopeptides from Bacillus and Pseudomonas: more than surfactants and antibiotics. *FEMS Microbiol Rev* **34**: 1037-1062.
Ramos-Montanez, S., H.C. Tsui, K.J. Wayne, J.L. Morris, L.E. Peters, F. Zhang, K.M. Kazmierczak, L.T. Sham & M.E. Winkler, (2008) Polymorphism and regulation of the spxB (pyruvate oxidase) virulence factor gene by a CBS-HotDog domain protein (SpxR) in serotype 2 Streptococcus pneumoniae. *Mol Microbiol* **67**: 729-746.
Robinson, M.D., D.J. McCarthy & G.K. Smyth, (2010) edgeR: a Bioconductor package for differential expression analysis of digital gene expression data. *Bioinformatics* **26**: 139-140.
Rocha-Estrada, J., A.E. Aceves-Diez, G. Guarneros & M. de la Torre, (2010) The RNPP family of quorum-sensing proteins in Gram-positive bacteria. *Appl Microbiol Biotechnol* **87**: 913-923.
Rutherford, S.T. & B.L. Bassler, (2012) Bacterial quorum sensing: its role in virulence and possibilities for its control. *Cold Spring Harb Perspect Med* **2**.
Sastalla, I., L.M. Maltese, O.M. Pomerantseva, A.P. Pomerantsev, A. Keane-Myers & S.H. Leppla, (2010) Activation of the latent PlcR regulon in Bacillus anthracis. *Microbiology* **156**: 2982-2993.

763 Slamti, L. & D. Lereclus, (2002) A cell-cell signaling peptide activates the PlcR virulence regulon
764 in bacteria of the Bacillus cereus group. *Embo J* **21**: 4550-4559.
765 Slamti, L. & D. Lereclus, (2005) Specificity and polymorphism of the PlcR-PapR quorum-
766 sensing system in the Bacillus cereus group. *J Bacteriol* **187**: 1182-1187.
767 Solomon, J.M., B.A. Lazazzera & A.D. Grossman, (1996) Purification and characterization of an
768 extracellular peptide factor that affects two different developmental pathways in Bacillus
769 subtilis. *Genes Dev* **10**: 2014-2024.
770 Sonenshein, A.L., (2007) Control of key metabolic intersections in Bacillus subtilis. *Nat Rev*
771 *Microbiol* **5**: 917-927.
772 Song, X.M., W. Connor, S. Jalal, K. Hokamp & A.A. Potter, (2008) Microarray analysis of
773 Streptococcus pneumoniae gene expression changes to human lung epithelial cells.
774 *Can J Microbiol* **54**: 189-200.
775 Trombe, M.C., G. Laneelle & A.M. Sicard, (1984) Characterization of a Streptococcus
776 pneumoniae mutant with altered electric transmembrane potential. *J Bacteriol* **158**:
777 1109-1114.
778 Trombe, M.C., M.A. Laneelle & G. Laneelle, (1979) Lipid composition of aminopterin-resistant
779 and sensitive strains of Streptococcus pneumoniae. Effect of aminopterin inhibition.
780 *Biochim Biophys Acta* **574**: 290-300.
781 van Opijnen, T. & A. Camilli, (2012) A fine scale phenotype-genotype virulence map of a
782 bacterial pathogen. *Genome Res* **22**: 2541-2551.
783 Waters, C.M. & B.L. Bassler, (2005) Quorum sensing: cell-to-cell communication in bacteria.
784 *Annual review of cell and developmental biology* **21**: 319-346.
785 Willey, J.M. & W.A. van der Donk, (2007) Lantibiotics: peptides of diverse structure and
786 function. *Annu Rev Microbiol* **61**: 477-501.
787 Yesilkaya, H., S. Manco, A. Kadioglu, V.S. Terra & P.W. Andrew, (2008) The ability to utilize
788 mucin affects the regulation of virulence gene expression in Streptococcus pneumoniae.
789 *FEMS Microbiol Lett* **278**: 231-235.
790 Zahner, D. & R. Hakenbeck, (2000) The Streptococcus pneumoniae beta-galactosidase is a
791 surface protein. *J Bacteriol* **182**: 5919-5921.

792

793

794 **Table 1**. Changes in relative transcript amounts caused by Δ*tprA* and Δ*phrA* mutations or the addition of the 10-residue synthetic
795 PhrA peptide[a]

Effect on expression & gene tag	Known or Predicted Function & Gene Name	+PhrA(10) vs. untreated[b]		Δ*tprA* vs. WT[c]		Δ(*tprA-phrA*) vs. WT[d]		Δ*phrA* vs. WT[e]	
		Log_2 fold change	FDR[f]	Log_2 fold change	FDR[f]	Log_2 fold change	FDR[f]	Log_2 fold change	FDR[f]
tprA, phrA gene region									
spd1744	lipoprotein, putative	2.7	3.0E-20	3.3	1.5E-27	3.2	5.0E-26		
spd1745	PlcR-family transcription factor, *tprA*	3.3	4.2E-88						
spd1746	Phr-family peptide signaling precursor protein, *phrA*	4.7	4.5E-81	5.0	3.7E-103	-4.0	2.4E-19	-4.5	9.1E-22
spd1747	lantibiotic precursor peptide	4.7	1.7E-133	4.7	5.3E-115	5.7	6.7E-217		
spd1748	lantibiotic precursor peptide	4.8	2.6E-80	4.8	2.5E-72	5.7	3.4E-123		
spd1749	bifunctional lantibiotic modification enzyme	3.5	4.3E-37	4.3	4.0E-52	3.9	3.8E-19		
spd1750	FAD-dependent flavoprotein	3.3	4.6E-35	4.2	2.2E-51	3.8	3.4E-24		
spd1751	membrane protein, putative	2.9	8.8E-17	3.8	1.1E-24	3.4	8.7E-14		
spd1752	toxin secretion ABC transporter, ATP-binding/permease protein	3.1	6.3E-18	4.0	1.4E-26	3.6	2.7E-13		
spd1753	serine protease, putative	3.0	4.3E-26	3.8	1.3E-37	3.4	1.3E-13		
spd1754	lantibiotic immunity protein	1.7	2.6E-15	2.4	3.2E-27	2.1	7.7E-11		
spd1755	ABC transporter, ATP-binding protein	1.7	4.4E-16	2.3	6.0E-24	2.0	4.9E-10		
spd1756	unknown	1.6	4.8E-05	2.5	2.7E-12	2.3	1.1E-09		
spd0769-0773 region									
spd0769	tmRNA, *ssrA*	2.0	1.5E-06						
spd0771	lactose phosphotransferase system repressor, *lacR1*	1.5	3.4E-14			1.1	1.4E-05		
spd0772	1-phosphofructokinase	1.6	7.7E-23			1.2	3.7E-12		
spd0773	PTS system fructose specific transporter subunit IIABC	1.5	1.5E-20			1.0	9.5E-06		

Other Genes							
spd0096	transcriptional regulator, PadR family protein	-1.1	3.4E-04				
spd0104	LysM domain-containing protein					-1.1	3.3E-05
spd0391	conserved hypothetical protein					0.99	2.1E-04
spd0450	type I restriction-modification system subunit S					-1.5	3.1E-06
spd0452	integrase/recombinase, phage integrase family protein					1.3	2.4E-04
spd0460	molecular chaperone, *dnaK*					-1.2	3.3E-05
spd2013	glycerol kinase, *glpK*				-1.1	1.8E-04	

[a] Strain construction, growth and RNA-Seq analysis are described in Experimental procedures. RNA was prepared from exponential cultures grown in BHI media at 37°C to OD_{620} ≈0.15 to 0.2. The Log_2 of the fold changes and FDR values are based on three independent biological replicates. Cut-offs for this table were 2.0-fold change and FDR value < 0.001. Empty boxes indicate that there was not a significant change in expression of a gene under one of the four conditions.

[b] The RNA transcript levels from strain IU1781 treated with 10 µM 10-residue synthetic PhrA compared to strain IU1781 receiving no treatment. The peptide was added to cells at an OD_{620} of 0.03 and then allowed to incubate to the required OD before harvesting.

[c] The RNA transcript levels from Δ*tprA* mutant strain IU4955 were compared to the RNA transcripts from an isogenic strain IU1781.

[d] The RNA transcript levels from Δ*tprA* Δ*phrA* mutant strain IU6118 were compared to the RNA transcripts from an isogenic strain IU1781.

[e] The RNA transcript levels from Δ*phrA* mutant strain IU4957 were compared to the RNA transcripts from an isogenic strain IU1781.

[f] FDR is the false-discovery rate (Benjamini & Hochberg, 1995).

FIGURE LEGENDS

Fig 1. TprA serves as an inhibitor of *phrA* expression.

(A) The effect of Δ*tprA* and Δ*phrA* mutations on *phrA-lacZ* expression. Strains: Spn007, "wild-type" parental strain used in this experiment; Spn013, Δ*tprA*; Spn019, Δ*phrA*; Spn195, Δ*tprA* CEP::TprA (complemented strain). Results shown are averages of 2-5 independent experiments and error bars depict the standard error of the mean. ***, significant at $P < 0.001$ compared to "wild type." +++, significant at $P < 0.001$ compared to Δ*tprA*. (B) *phrA* mRNA levels in a Δ*tprA* mutant strain. Strains: IU1781 & Spn049, "wild-type" parental strains used in this experiment; Spn052, Δ*tprA*; Spn197, Δ*tprA* CEP::TprA (complemented strain). mRNA levels were normalized to 16S RNA levels, from 2 independent experiments, and are shown as a ratio relative to the wild-type levels. Error bars depict the standard error of the mean. *, significant at $P < 0.05$ compared to "wild type." +, significant at $P < 0.05$ compared to Δ*tprA*. Different parent strains were used in these approaches containing wild-type alleles for the genes of interest.

Fig 2. Identification of the minimal PhrA-signaling peptide.

(A) *phrA-lacZ* reporter expression is elevated when the full length *phrA* gene is overexpressed. Strains: Spn065, full length PhrA; Spn191, PhrAΔ42-56 ; Spn189, PhrAΔ47-56 ; Spn187, PhrAΔ52-56 ; Spn243, PhrAΔ56 . Cells were grown in BHI or BHI+1% fucose (inducer) to mid-exponential phase (OD_{620} of between 0.15 to 0.35) when samples were removed for β-galactosidase activity assays. Results shown are the averages of at least 3 independent replicates and error bars indicate the standard error of the mean for each set. ***, significant at $P < 0.001$ compared to uninduced strain containing the full-length PhrA construct. (B) Synthetic peptides corresponding to the C-terminus of PhrA used in (C) below. (C) Induction of the *phrA-lacZ* reporter was observed when cells were treated with the last 6, 7, or 10 amino acids of PhrA. Early exponential phase (OD_{620} of ~0.1) wild-type cells (Spn007) were incubated with

synthetic peptides at a final concentration of 5 μM or peptide-resuspension buffer for two hours prior to analysis by β-galactosidase assays. Results shown are the averages of at least 3 independent replicates and error bars indicate the standard error of the mean for each set. *, significant at $P < 0.05$ and **, significant at $P < 0.01$ compared to the "wild type" strain incubated with buffer.

Fig 3. Oligopeptide permease is required for induction of *phrA-lacZ* in response to synthetic peptide.

Strains lacking *amiC* in a wild-type or a Δ*tprA* mutant background were tested for their ability to induce *phrA-lacZ* expression in response to the 10-residue PhrA peptide. Strains: Spn007, "wild-type" parental strain used in this experiment; Spn013, Δ*tprA*; Spn141, Δ*amiC*; Spn165, Δ*tprA* Δ*amiC*. Early exponential phase cells (OD_{620} of ~0.1) grown in BHI were incubated with 5 μM synthetic peptide or peptide-resuspension buffer for two hours prior to analysis by β-galactosidase activity assays. Results shown are the average of at least two independent trials, and error bars represent the standard error of the mean. ***, significant at $P < 0.001$ compared to the strain treated with buffer.

Fig 4. PhrA can signal between cells when grown to high cell density in media containing galactose.

Cells (Spn007, wild-type) grown in CDM-glucose (closed squares) or CDM-galactose (open circles). Panel A shows a representative growth curve of these cells on these media. Note that after inoculation of the cultures several hours pass before there is a measurable level of cells, and this lag phase is longer in CDM-galactose. Panel B shows expression of *phrA-lacZ* in the Spn007 cells. At least two independent experiments were performed; the results from one representative experiment are shown. Panel C shows induction of *phrA-lacZ* when these were

857 resuspended in conditioned media from wild-type cells (IU1781) compared to untreated media,
858 and no induction was observed in conditioned media from cells lacking *phrA* (IU4957). The
859 results shown are the average of at least two independent trials and the error bars depict the
860 standard error of the mean. *, significant at $P < 0.05$ compared to untreated media. +, significant
861 at $P < 0.05$ compared to wild-type conditioned media.
862
863 **Fig 5. The TprA/PhrA system regulates a putative lantibiotic biosynthesis operon.**
864 ORFs are represented by dark grey arrows (in the case of the TprA/PhrA system) or light gray
865 arrows (for the putative lantibiotic biosynthesis genes) and the D39 gene identification numbers
866 are indicated in the arrows, with genes spd1747 and spd1748 shorten to 47 and 48,
867 respectively. Known or predicted functions of each gene are indicated above the arrows, and --
868 indicates that the function of the genes is unknown. The putative promoters, predicted by the
869 results with RNA-seq, are represented by bent black arrows, and putative promoters predicted
870 by the DOOR database are shown as bent gray arrows. Small black boxes are predicted CRE-
871 binding sites of CcpA (Carvalho *et al.*, 2011). Genes whose expression has been found to be
872 increased in either a Δ*tprA* mutant or by the addition of the PhrA peptide are denoted by + under
873 the gene.
874
875 **Fig 6. Model for the mechanism by which PhrA and TprA control gene expression in *S.***
876 ***pneumoniae*.**
877 The mature PhrA peptide is encoded by *phrA* producing a precursor protein in the absence of
878 glucose. Glucose repression occurs through a CRE element that is in *phrA* promoter region.
879 The PhrA precursor is exported and processed to release the mature PhrA peptide (dark gray,
880 small ovals). When at a sufficient concentration, the PhrA peptide interacts with oligopeptide
881 permease and is transported into the cell where it inhibits the activity of TprA leading to de-
882 repression of *phrA, tprA,* and a change in transcription of lantibiotic genes (wide arrows). Only

three of the eight lantibiotic biosynthesis cluster genes are shown here for simplicity (black outlined, wide arrows with one not shown to scale (angled lines)). Bent arrows indicate the location of data-supported (black) or predicted (gray) promoters, all of which are negatively regulated by TprA (denoted by lines that end with a horizontal line).

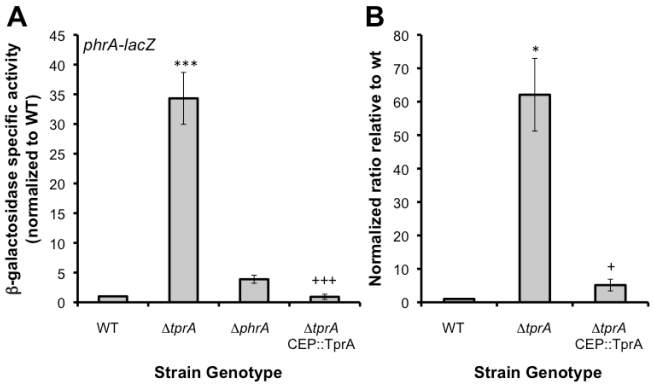

876

877 Figure 1

878

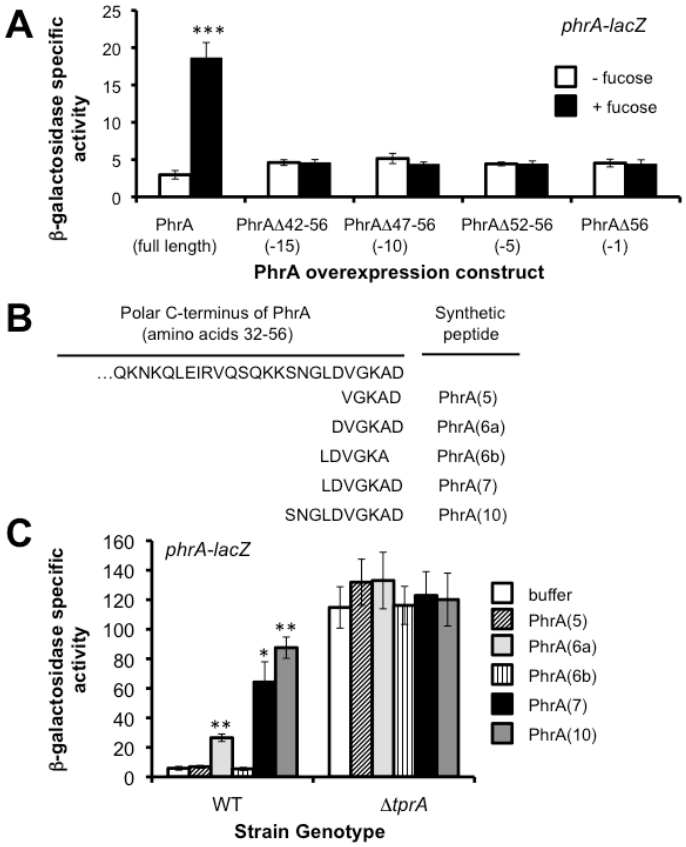

878

879 Figure 2

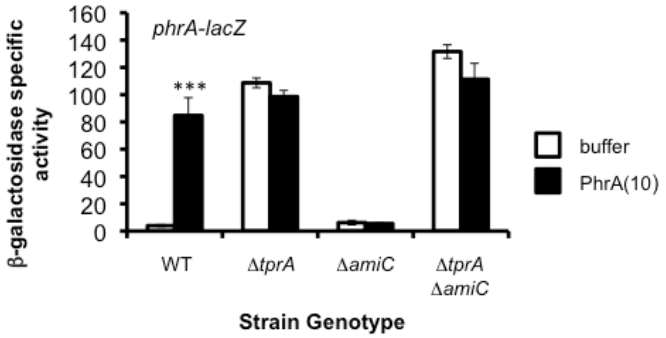

880

881 Figure 3

882

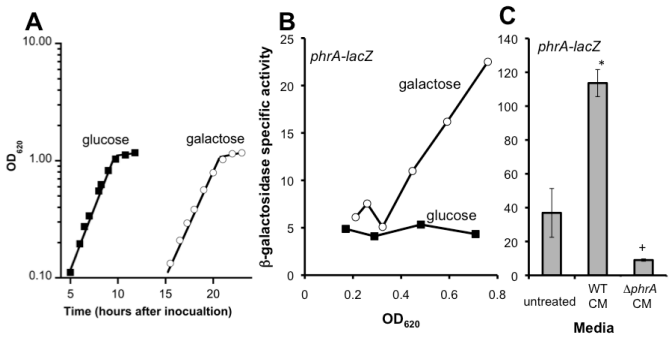

882

883 Figure 4

884

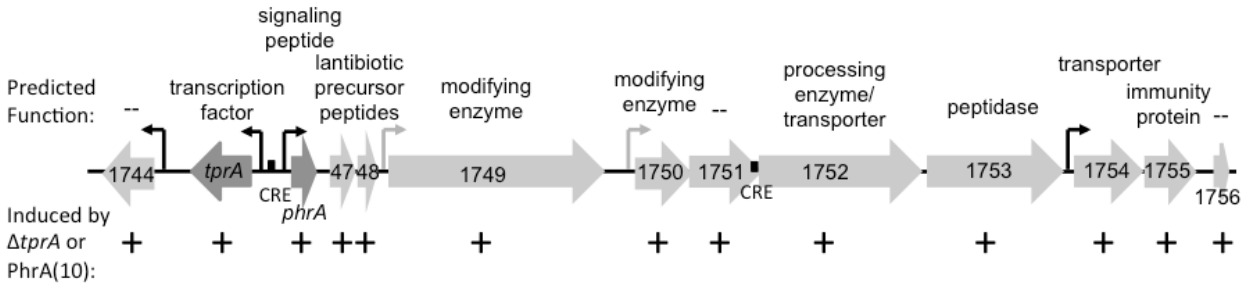
Predicted Function:
--
transcription factor
signaling peptide
lantibiotic precursor peptides
modifying enzyme
modifying enzyme
--
processing enzyme/ transporter
peptidase
transporter
immunity protein
--
1744
tprA
CRE
phrA
1748
1749
1750
1751
CRE
1752
1753
1754
1755
1756
Induced by ΔtprA or PhrA(10):

Figure 5

886

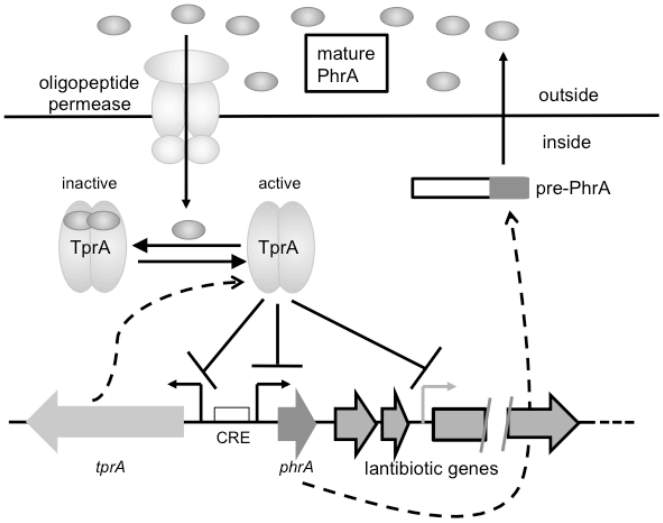

887

888 Figure 6

Supplemental Information:

Supplemental Materials and Methods: Bioinformatic identification of Phr peptide cassettes in Streptococci; Murine pneumonia model of infection; Construction and verification of mutants and constructs; Peptide synthesis and purification; Modeling the Structure of TprA

Table S1: Putative Phr peptide signaling cassettes with similarity to TprA/PhrA identified in Streptococci.

Table S2: Putative Phr peptide signaling cassettes with similarity to TprB/PhrB identified in Streptococci.

Table S3: Putative Phr peptide signaling cassettes with similarity to TprC/PhrC identified in Streptococci.

Table S4: Top 10 Structures predicted to match TprA of *S. pneumoniae*.

Table S5: Strains used in this study.

Table S6: Oligos synthesized for this study.

Table S7: Assembly of gene constructs used in this study.

Figure S1: Structural model of a monomer of TprA.

Figure S2: Deletion of *tprA* or *phrA* does not alter physiology compared to wild-type.

Figure S3: qRT-PCR confirmation of induction of *phrA* expression by the 10-residue PhrA peptide.

Figure S4: qRT-PCR confirmation of induction of *phrA* expression in CDM-galactose.

Figure S5: qRT-PCR confirmation of TprA/PhrA dependent regulation of select lantibiotic biosynthesis genes.

Figure S6: *tprA/phrA* JBrowse snapshot.

SUPPLEMENTAL MATERIALS AND METHODS

Bioinformatic identification of Phr peptide cassettes in Streptococci

The protein sequences from the Rap proteins (RapA-K) in *B. subtilis* and PlcR from the *B. cereus* group were subjected to tblastn analysis at NCBI (http://blast.ncbi.nlm.nih.gov/Blast.cgi?CMD=Web&PAGE_TYPE=BlastHome) with the organism search set limited to Streptococcus (taxid: 1301). A second round of tblastn searches were performed to enlarge the pool of potential cassettes with the three putative PlcR homologues that were adjacent to open reading frames encoding a protein of 30 to 100 amino acids in the TIGR4 strain of *S. pneumoniae* (SP_1946, SP_1057, and SP_0163). The hits with an E value (significance) of < 1*10^-9, corresponding to the initial E value obtained in the tblastn analysis with PlcR of *B. cereus*, were placed into 3 different groups based on their similarity to each of the PlcR homologues from TIGR4. This method ensured that only homologues with significant similarity were maintained and duplicate hits were removed. To ensure identification of a greater number of putative Phr

peptide encoding genes, the Phr peptide encoding proteins (SP_1947, SP_1058, and SP_0164) were subjected to tblastn analysis and matched to their corresponding PlcR homologue. The systematic name for the PlcR homologues and the adjacent small gene predicted to encode the Phr peptide were then identified or the location on the chromosome determined. For those cassettes where the Phr peptide encoding gene was not annotated, ambiguous, or missing, the intergenic regions between the PlcR homologue and the upstream and downstream genes were obtained and subjected to gene prediction analysis using GeneMark.hmm (http://exon.gatech.edu/gmhmm2_prok.cgi) with the species set to TIGR4 (Lukashin & Borodovsky, 1998). The gene prediction results were then correlated to the tblastn analysis results, where possible. For annotation, the predicted Phr peptide encoding gene needed to encode a protein of between 30 and 100 amino acids and have a discernable start and stop codon.

Murine pneumonia model of infection

All procedures were approved in advance by the Institutional Animal Care and Use Committee and were performed according to recommendations of the National Research Council. Procedures were carried out as described previously (Gutu *et al.*, 2010, Kazmierczak *et al.*, 2009) except that cells were harvested at an OD_{620} of ~0.17 and ~2.0 x 10^4 CFU were found in the 50 µl inoculum. Mice were monitored at 4-6 hour intervals. Death was not used as an endpoint. Moribund mice were euthanized by CO_2 asphyxiation, and that time point was used as the "time of death" in the survival curves. Kaplan-Meier survival curves and log-rank tests were generated by GraphPad Prism software.

Construction and verification of mutants and constructs

Strains containing antibiotic markers were constructed by transforming linear DNA amplicons into competent pneumococcal cells as described previously (Ng *et al.*, 2003, Robertson *et al.*, 2002). These amplicons were synthesized by overlapping fusion PCR using Phusion High-Fidelity Master Mix (NEB) or KOD Hot Start DNA Polymerase (Novagen). Primers and constructs synthesized for this study are listed in Tables S6 and S7. Markerless mutations were introduced into the *S. pneumoniae* genome using the Janus method of allelic replacement in strains containing *rpsL1* (Str^R) as initially described in (Sung *et al.*, 2001). All mutations were confirmed by allele size verification and DNA sequencing. Strains containing the *amiC*(spd1670)<>*erm* allele have the open reading frame of *amiC* replaced with P_c-*erm*. Strains containing Δ*tprA*::(*kan rpsL*$^+$), Δ*tprA*::(P_c-*erm*), Δ*phrA*::(*kan rpsL*$^+$), or Δ*phrA*::(P_c-*erm*) have replaced amino acids 21 to 268 of *tprA* or amino

acids 21 to 37 of *phrA* with the Janus cassette (*kan rpsL*$^+$) or P_c-*erm*. The unmarked Δ*tprA* mutant strains contain an in-frame deletion of amino acids 21 to 268 (out of 287 amino acids total). The unmarked Δ*phrA* mutant strains have the first 9 nucleotides fused to the final 14 nucleotides of *phrA*. Strains containing Δ(*tprA-phrA)*::(*kan rpsL*$^+$) replace the 5' end of both genes and the intervening promoter region with the Janus cassette (*kan rpsL*$^+$) and maintain 60 nucleotides from the 3' end of both *tprA* and *phrA*. The unmarked Δ(*tprA-phrA*) mutant strain contains a deletion from base 804 of *tprA* to base 112 of *phrA* (with the first base of the start codon being base 1). For overexpression of PhrA, the open reading frame corresponding to full length (all 56 residues) or the PhrA truncations (lacking the last 1, 5, 10 or 15 residues) were placed under the control of a fucose-inducible promoter (P_{fcsK}) and integrated at the chromosomal expression platform (CEP), a transcriptionally silent locus that was previously determined to be suitable for ectopic expression in *S. pneumoniae* (Guiral *et al.*, 2006, Biller *et al.*, 2011). The Δ*tprA* complemented strains contained the open reading frame for *tprA* under the control of its own promoter integrated at CEP. Intermediate constructs CEP::(*kan rpsL*$^+$) (Tsui *et al.*, 2011) or CEP::(*erm rpsL*$^+$) (this study) were used in the Janus method of allelic replacement to integrate markerless constructs at CEP.

To create the *phrA-lacZ* reporter construct, the intergenic region between *phrA* and *tprA* (P_{phrA}) was cloned using a modified overlapping fusion PCR protocol into pPP2, which contains a promoterless hybrid β-galactosidase gene that is flanked by regions of the *S. pneumoniae bgaA* gene (Halfmann *et al.*, 2007). The P_{phrA} promoter was amplified using primers BL1454 and BL1455, which each encode homology to pPP2. The pPP2 integration plasmid was linearized by double digest with BamHI and SphI, and then used in a PCR sewing reaction with the P_{phrA} PCR product. The resulting plasmid (pBL915) was transformed into pneumococcal strains, and the subsequent integration event created the allele *bgaA*::(*tet* P_{phrA}-*lacZ*) that inactivates the endogenous pneumococcal β-galactosidase. The *bgaA*::(*tet* P_{phrA}-*lacZ*) allele was confirmed by PCR amplification and DNA sequencing of transformed cells.

Peptide synthesis and purification

Peptides were synthesized using 0.2 mmol of 4-hydroxymethyl-phenylacetamidomethyl (PAM) resin (Midwest Biotech) on a modified Applied Biosystems 430A peptide synthesizer. The solid phase peptide synthesis protocol utilized in situ neutralization for Boc-chemistry as described by Schnolzer et al. (Schnolzer *et al.*, 1992). Amino acids (Midwest Biotech) were side chain protected with the following groups: Asp(OcHex),

Asn(Xan), His(BOM), Lys(2-Cl-Z), Ser(Bzl), Thr(Bzl). Activation of amino acids (2 mmol) was performed with 0.5M 3-(diethoxyphosphoryloxy)-1, 2, 3-benzotriazin-4(3H)-one and diisopropylethylamine (4:1 v/v). Completed peptidyl-resins were treated with HF/p-cresol (10:0.5 v/v) at 0° C for 1 hour. The HF was removed *in vacuo* and the deprotected peptide was precipitated and washed in diethyl ether. The peptide was dissolved in 20% acetonitrile/1% acetic acid and lyophilized. The sequence of the five individual peptide C-terminal acids were: SNGLDVGKAD – PhrA(10), LDVGKAD – PhrA(7), DVGKAD – PhrA(6A), LDVGKA – PhrA(6B), and VGKAD – PhrA(5).

Reversed phase HPLC (RP-HPLC) was utilized for peptide purification. A C18 stationary phase (Vydac 218TP, 250X22 mm, 10 µm) was employed with a linear acetonitrile gradient in 0.1% TFA during the preparative RP-HPLC purification. Analytical analysis was performed on peak fractions by employing RP-HPLC with a C8 column (Zorbax 300SB, 4.6X50 mm, 3.5 µm). Peptide identity and purity was assessed by analytical HPLC and ESI- or MALDI-MS. Lyophilized peptides were stored at 4°C. All peptides were found to have the correct molecular weight and were >95% pure.

Modeling the Structure of TprA

The primary sequence for TprA from *S. pneumoniae* D39 was inputted into the Phyre website (http://www.sbg.bio.ic.ac.uk/phyre)(Kelley & Sternberg, 2009) and 1000 homologues were detected with the pseudo-multiple sequence alignment (see Table S7 for a list of the top 10 matching protein structures). All 1000 homologues obtained had an E value of 6e-11 or lower and also showed a high degree of sequence diversity (between 5-20% sequence identity), suggesting high confidence in the structural prediction. TprA is predicted to consist of 14 helices interspersed with coil regions. 12 of the 14 helices had high confidence values (scores of 8 or 9 throughout). 2 of the 14 helices – helices 3 and 5 – have lower confidence values (scores of 5 to 8). A strong alignment match was found to PlcR of *B. thuringiensis*, with the 3-D structural model (Figure S6) predicted to be accurate throughout the alignment.

Search for putative TprA-binding sites

To identify possible TprA binding sites, we based our search on the consensus PlcR-binding site of *Bacillus cereus* (Gohar et al., 2008). This site is an inverted repeat of 16 nucleotides, with the outermost 4 nucleotides playing the most important role in PlcR binding. We search the 500 bases upstream of the start codon of the following genes for inverted repeats: *tprA*, *phrA*, spd0771, spd1749, spd1750, and spd1754.

Each upstream region was analyzed by Palindrome (http://emboss.bioinformatics.nl/cgi-bin/emboss/help/palindrome) with the minimum and maximum length of palindrome set to 8 nucleotides (i.e. ½ of the inverted repeat), the maximum gap between repeated regions set to zero nucleotides, and up to 4 mismatches were allowed. As an example, 25 inverted repeats were identified upstream of *phrA*. These repeats were then screened manually for the location of the mismatches, and only three of the 25 inverted repeats had a run of at least three matches at the outer ends of the repeat. Matches to these three inverted repeats were searched for by Blast in the promoter regions of the other genes, and no significant matches were identified.

REFERENCES

Biller, S.J., K.J. Wayne, M.E. Winkler & W.F. Burkholder, (2011) The putative hydrolase YycJ (WalJ) affects the coordination of cell division with DNA replication in Bacillus subtilis and may play a conserved role in cell wall metabolism. *J Bacteriol* **193**: 896-908.

Gohar, M., K. Faegri, S. Perchat, S. Ravnum, O.A. Okstad, M. Gominet, A.B. Kolsto & D. Lereclus, (2008) The PlcR virulence regulon of Bacillus cereus. *PLoS One* **3**: e2793.

Guiral, S., V. Henard, M.H. Laaberki, C. Granadel, M. Prudhomme, B. Martin & J.P. Claverys, (2006) Construction and evaluation of a chromosomal expression platform (CEP) for ectopic, maltose-driven gene expression in Streptococcus pneumoniae. *Microbiology* **152**: 343-349.

Gutu, A.D., K.J. Wayne, L.T. Sham & M.E. Winkler, (2010) Kinetic characterization of the WalRKSpn (VicRK) two-component system of Streptococcus pneumoniae: dependence of WalKSpn (VicK) phosphatase activity on its PAS domain. *J Bacteriol* **192**: 2346-2358.

Halfmann, A., R. Hakenbeck & R. Bruckner, (2007) A new integrative reporter plasmid for Streptococcus pneumoniae. *FEMS Microbiol Lett* **268**: 217-224.

Kazmierczak, K.M., K.J. Wayne, A. Rechtsteiner & M.E. Winkler, (2009) Roles of rel(Spn) in stringent response, global regulation and virulence of serotype 2 Streptococcus pneumoniae D39. *Mol Microbiol* **72**: 590-611.

Kelley, L.A. & M.J. Sternberg, (2009) Protein structure prediction on the Web: a case study using the Phyre server. *Nat Protoc* **4**: 363-371.

Lanie, J.A., W.L. Ng, K.M. Kazmierczak, T.M. Andrzejewski, T.M. Davidsen, K.J. Wayne, H. Tettelin, J.I. Glass & M.E. Winkler, (2007) Genome sequence of Avery's virulent serotype 2 strain D39 of Streptococcus pneumoniae and comparison with that of unencapsulated laboratory strain R6. *J Bacteriol* **189**: 38-51.

Lukashin, A.V. & M. Borodovsky, (1998) GeneMark.hmm: new solutions for gene finding. *Nucleic Acids Res* **26**: 1107-1115.

Ng, W.L., G.T. Robertson, K.M. Kazmierczak, J. Zhao, R. Gilmour & M.E. Winkler, (2003) Constitutive expression of PcsB suppresses the requirement for the essential VicR (YycF) response regulator in Streptococcus pneumoniae R6. *Mol Microbiol* **50**: 1647-1663.

Ramos-Montanez, S., H.C. Tsui, K.J. Wayne, J.L. Morris, L.E. Peters, F. Zhang, K.M. Kazmierczak, L.T. Sham & M.E. Winkler, (2008) Polymorphism and regulation of the spxB (pyruvate oxidase) virulence factor gene by a CBS-HotDog domain protein (SpxR) in serotype 2 Streptococcus pneumoniae. *Mol Microbiol* **67**: 729-746.

Robertson, G.T., W.L. Ng, J. Foley, R. Gilmour & M.E. Winkler, (2002) Global transcriptional analysis of clpP mutations of type 2 Streptococcus pneumoniae and their effects on physiology and virulence. *J Bacteriol* **184**: 3508-3520.

Schnolzer, M., P. Alewood, A. Jones, D. Alewood & S.B. Kent, (1992) In situ neutralization in Boc-chemistry solid phase peptide synthesis. Rapid, high yield assembly of difficult sequences. *Int J Pept Protein Res* **40**: 180-193.

Skinner, M.E., A.V. Uzilov, L.D. Stein, C.J. Mungall & I.H. Holmes, (2009) JBrowse: a next-generation genome browser. *Genome research* **19**: 1630-1638.

Sung, C.K., H. Li, J.P. Claverys & D.A. Morrison, (2001) An rpsL cassette, janus, for gene replacement through negative selection in Streptococcus pneumoniae. *Appl Environ Microbiol* **67**: 5190-5196.

Tsui, H.C., S.K. Keen, L.T. Sham, K.J. Wayne & M.E. Winkler, (2011) Dynamic distribution of the SecA and SecY translocase subunits and septal localization of the HtrA surface chaperone/protease during Streptococcus pneumoniae D39 cell division. *MBio* **2**.

Tsui, H.C., D. Mukherjee, V.A. Ray, L.T. Sham, A.L. Feig & M.E. Winkler, (2010) Identification and characterization of noncoding small RNAs in Streptococcus pneumoniae serotype 2 strain D39. *Journal of bacteriology* **192**: 264-279.

Table S1. Putative Phr peptide signaling cassettes with similarity to TprA/PhrA identified in Streptococci.

Strain	Serotype[1]	TprA[2]	PhrA[2]
Streptococcus pneumoniae R6	no capsule	spr1763	spr1764
Streptococcus pneumoniae D39	2	SPD_1745	SPD_1746
Streptococcus pneumoniae TIGR4	4	SP_1946	SP_1947
Streptococcus pneumoniae ATCC 700669	23F	SPN23F19680	SPN23F19690
		SPN23F12750	SPN23F12740
Streptococcus pneumoniae JJA	14	SPJ_1940	SPJ_1941
Streptococcus pneumoniae SPN994038	3	SPN994038_17070	SN994038_17080
Streptococcus pneumoniae SPN994039	3	SPN994039_17080	SN994039_17090
Streptococcus pneumoniae OXC141	3	SPNOXC17140	SPNOXC17150
Streptococcus pneumoniae SPN034183	3	SPN034183_17180	SPN034183_17190
Streptococcus pneumoniae P1031	1	SPP_1974	SPP_1975
Streptococcus pneumoniae 670-6B	6B	SP670_2033	SP670_2034
Streptococcus pneumoniae AP200	11A	SPAP_1965	1833450-1833500*
Streptococcus pneumoniae Hungary19A-6	19A	SPH_2095	1930248-1930430
Streptococcus pneumoniae INV200	14	SPNINV200_17660	SPNINV200_17670
Streptococcus pneumoniae CGSP14	14	SPCG_1919	SPCG_1920
Streptococcus pneumoniae gamPNI0373	1	HMPREF1038_01936	1766716-1766766*
Streptococcus pneumoniae SPN034156	3	SPN034156_07950	SPN034156_07960
Streptococcus pneumoniae SPNA45	3	SPNA45_00262	SPNA45_00261
Streptococcus pneumoniae 70585	5	SP70585_2025	SP70585_2026
Streptococcus pseudopneumoniae IS7493	no capsule	SPPN_10015	SPPN_10020
		SPPN_10040	SPPN_10045
Streptococcus sp. I-G2		N596_03305	N596_03300
Streptococcus parasanguinis FW213		Spaf_1866	Spaf_1865
Streptococcus pneumoniae TCH8431/19A	19A	HMPREF0837_12189	HMPREF0837_12190
Streptococcus pneumoniae A026	19F	T308_09020	T308_09025
Streptococcus pneumoniae Taiwan19F-14	19F	SPT_1904	SPT_1905
Streptococcus pneumoniae ST556	19F	MYY_1854	MYY_1855
Streptococcus mitis B6		smi_1349	
Streptococcus pneumoniae G54	19F	SPG_1855	1768003-1768185

		SPG_1247	SPG_1246
Streptococcus pneumoniae SPN032672	1	1146774-1147634	1146585-1146418*
Streptococcus pneumoniae SPN033038	1	859429-858569	859618-859785*
Streptococcus pneumoniae INV104	1	INV104_16780	INV104_16790
Streptococcus pneumoniae Pn19, partial integrative and conjugative element ICE6094	3	11503-12303	11247-11080*
Streptococcus dysgalactiae subsp. equisimilis GGS 124		SDEG_1334	1287044-1286877
Streptococcus iniae SF1	I	K710_0479	450126-450332
Streptococcus suis S735	2	YYK_01050	
Streptococcus suis P1/7	1	SSU0226	
Streptococcus suis A7	2	SSUA7_0224	
Streptococcus suis GZ1	2	SSGZ1_0221	
Streptococcus suis SS12	1/2	SSU12_0228	
Streptococcus suis SC84	7	SSUSC84_0215	
Streptococcus suis SC070731	2	NJAUSS_0239	
Streptococcus suis JS14	14	SSUJS14_0231	
Streptococcus suis BM407	1	SSUBM407_0217	
Streptococcus suis TL13	16	TL13_0270	
Streptococcus suis D12	9	SSUD12_0220	
Streptococcus suis D12	9	SSUD12_0266	
Streptococcus suis ST1	1	SSUST1_0238	
Streptococcus suis 05ZYH33	2	SSU05_0241 SSU05_0242	
Streptococcus suis 98HAH33	2	SSU98_0237 SSU98_0238	
Streptococcus gallolyticus UCN34		GALLO_2166	
Streptococcus gallolyticus subsp. gallolyticus ATCC 43143		SGGB_2148	
Streptococcus gallolyticus subsp. gallolyticus ATCC BAA-2069		SGGBAA2069_c21620	

[1]Serotype of Streptococcal strain (where known).

[2]The gene numbers for the annotated genes with similarity to TprA and PhrA are indicated. Number ranges indicate the chromosomal position of putative genes, which were predicted with GeneMark.hmm (Lukashin A. and Borodovsky M., NAR, 1998, 26:1107-1115). The lack of a gene number or chromosomal position indicates that no ortholog of PhrA was identified.

* Indicates that these putative Phr genes may be non-functional, as they are only predicted to be 17-residues long and do not have a full signal sequence.

Table S2. Putative Phr peptide signaling cassettes with similarity to TprB/PhrB identified in Streptococci.

Strain	Serotype[1]	TprB[2]	PhrB[2]
Streptococcus pneumoniae PN1, transposon ICESpPN1	6	35661-36527	36680-36814
Streptococcus pneumoniae TIGR4	4	SP_1057	SP_1058
Streptococcus intermedius B196		SIR_0232	218928-219020
Streptococcus anginosus subsp. whileyi MAS624		ANG_2094	2077585-2077493
Streptococcus anginosus C238		SANR_0179	158936-159028
Streptococcus equi subsp. zooepidemicus MGCS10565		Sez_1897	

[1]Serotype(s) of Streptococcal strains (where known).

[2]The gene numbers for the annotated genes with similarity to TprB and PhrB are indicated. Number ranges indicate the chromosomal position of putative genes, which were predicted with GeneMark.hmm (Lukashin A. and Borodovsky M., NAR, 1998, 26:1107-1115). The lack of a gene number or chromosomal position indicates that no ortholog of PhrB was identified.

Table S3. Putative Phr peptide signaling cassettes with similarity to TprC/PhrC identified in Streptococci.

Strain	Serotype[1]	TprC[2]	PhrC[2]
Streptococcus pneumoniae TIGR4, complete genome	4	SP_0163	SP_0164
Streptococcus pneumoniae SPN032672 draft genome	1	1323430-1324293	1324449-1324577
Streptococcus pneumoniae SPN032672 draft genome	1	1619009-1619881	
Streptococcus pneumoniae SPN033038 draft genome	1	1324748-1325614	1325766-1325894
Streptococcus pneumoniae SPN033038 draft genome	1	1621196-1622068	
Streptococcus pneumoniae INV104 genome	1	INV104_01370	158461-158589
Streptococcus pneumoniae INV104 genome	1	INV104_04140	
Streptococcus pneumoniae 670-6B, complete genome	6B	SP670_0243	SP670_0244
Streptococcus mitis B6 complete genome, strain B6		smi_1259	
Streptococcus suis SS12, complete genome	1/2	SSU12_0860	SSU12_0859
Streptococcus thermophilus JIM 8232 complete genome		STH8232_0692	STH8232_0693
Streptococcus thermophilus LMD-9, complete genome		STER_1693	
Streptococcus pseudopneumoniae IS7493, complete genome	no capsule	SPPN_02890	
Streptococcus anginosus C1051, complete genome		SAIN_1577	
Streptococcus constellatus subsp. pharyngis C818, complete genome		SCR2_0260	251988-252113
Streptococcus constellatus subsp. pharyngis C232, complete genome		SCRE_0260	251988-252113
Streptococcus constellatus subsp. pharyngis C1050, complete genome		SCI_0280	270033-270158
Streptococcus iniae SF1, complete genome	I	K710_0690	
Streptococcus suis TL13, complete genome	16	TL13_1797	1825482-1825360
Streptococcus suis D9, complete genome	7	SSUD9_2017	SSUD9_2016

[1]Serotype(s) of Streptococcal genome (where known).

[2]The gene numbers for the annotated genes with similarity to TprB and PhrB are indicated. Number ranges indicate the chromosomal position of putative genes, which were predicted with GeneMark.hmm (Lukashin A. and Borodovsky M., NAR, 1998, 26:1107-1115). The lack of a gene number or chromosomal position indicates that no ortholog of PhrB was identified.

Table S4. Top 10 Structures predicted to match TprA of *S. pneumoniae*.

Protein[1]	Species	PDB ID[2]	E-value
PlcR	*B. thuringiensis*	2QFC	1.60E-23
Tom70	*S. cerevisiae*	2GW1	1.10E-14
gamma-SNAP	*D. rerio*	2IFU	3.50E-14
TPR Domain of OGT	*H. sapiens*	1W3B	2.30E-13
TPR domain of PEX5	*H. sapiens*	1FCH	2.50E-13
YrrB	*B. subtilis*	2Q7F	3.30E-13
PilF	*P. aeruginosa*	2FI7	2.30E-12
8-repeat consensus TPR superhelix	Synthetic protein	2HYZ	2.90E-11
TTC0263	*T. thermophilus*	2PL2	3.10E-11

[1] Protein structures that were identified as similar in the Protein Domain Database.

[2] Protein Domain Database identifiers (http://www.rcsb.org/pdb/home/home.do).

Table S5: Strains used in this study

Strain	Relevant Genotype[1]	Antibiotic resistance[2]	Reference or Source[3]
E012	Δ*cps* Δ*amiC*(spd1670)<>*erm*	Erm	*amiC*<>*erm* x IU1945
E294	Δ*cps* Δ*tprA*::(P_c-*erm*)	Erm	Δ*tprA*::(P_c-*erm*) x IU1945
E295	Δ*cps* Δ*phrA*::(P_c-*erm*)	Erm	Δ*phrA*::(P_c-*erm*) x IU1945
IU1690	Wild-type D39 parent	none	(Lanie *et al.*, 2007)
IU1781	*rpsL1*	Str	(Ramos-Montanez *et al.*, 2008)
IU1912	spd1717::(*kan* Tn4001 *luxABCDE)*	Kan	(Ramos-Montanez *et al.*, 2008)
IU1945	Δcps	none	(Lanie *et al.*, 2007)
IU3116	*rpsL1* CEP::(*kan rpsL*$^+$)	Kan	(Tsui *et al.*, 2011)
IU3131	*rpsL1* CEP::(P_{fcsK}-*vicK* Δ*vicK)*	Str	Winkler lab stock
IU4920	Δ*tprA*::(P_c-*erm*)	Erm	E294 x IU1690
IU4922	Δ*phrA*::(P_c-*erm*)	Erm	E295 x IU1690
IU4924	*rpsL1* Δ*tprA*::(*kan rpsL*$^+$)	Kan	K282 x IU1781
IU4926	*rpsL1* Δ*phrA*::(*kan rpsL*$^+$)	Kan	K284 x IU1781
IU4955	*rpsL1* Δ*tprA*	Str	Δ*tprA* x IU4924
IU4957	*rpsL1* Δ*phrA*	Str	Δ*phrA* x IU4926
IU6066	*rpsL1 Δ(tprA-phrA)::(kan rpsL*$^+$*)*	Kan	*ΔtprA ΔphrA::(kan rpsL*$^+$*)* x IU1781
IU6118	*rpsL1 Δ(tprA-phrA)*	Str	*ΔtprA ΔphrA* x IU6066
K282	Δ*cps* Δ*tprA*::(*kan rpsL*$^+$)	Kan	Δ*tprA*::(P_c-*kan*^{R}-*rpsL*$^+$) x IU1945
K284	Δ*cps* Δ*phrA*::(*kan rpsL*$^+$)	Kan	Δ*phrA*::(P_c-*kan*^{R}-*rpsL*$^+$) x IU1945
Spn007	*rpsL1* Δ*bgaA*::(*tet* P_{phrA}-*lacZ*)	Str, Tet	pBL915 x IU1781
Spn013	*rpsL1* Δ*tprA* Δ*bgaA*::(*tet* P_{phrA}-*lacZ*)	Str, Tet	pBL915 x IU4955
Spn019	*rpsL1* Δ*phrA* Δ*bgaA*::(*tet* P_{phrA}-*lacZ*)	Str, Tet	pBL915 x IU4957
Spn037	*rpsL1* Δ*tprA* CEP::(*kan rpsL*$^+$)	Kan	IU3116 x IU4955
Spn041	*rpsL1* Δ*bgaA*::(*tet* P_{phrA}-*lacZ*) CEP::(*kan rpsL*$^+$)	Kan, Tet	IU3116 x Spn007
Spn049	*rpsL1* SPD_1717::(*kan* Tn4001 *luxABCDE*)	Str, Kan	IU1912 x IU1781
Spn052	*rpsL1* Δ*tprA* spd1717::(*kan* Tn4001 *luxABCDE*)	Str, Kan	IU1912 x IU4955
Spn053	*rpsL1* Δ*phrA* spd1717::(*kan* Tn4001 *luxABCDE*)	Str, Kan	IU1912 x IU4957
Spn065	*rpsL1* Δ*bgaA*::(*tet* P_{phrA}-*lacZ*) CEP::(P_{fcsK}-*phrA*)	Str, Tet	CEP::(P_{fcsK}-*phrA*) x Spn041
Spn075	*rpsL1* Δ*tprA* CEP::(P_{tprA}-*tprA*)	Str	CEP::(P_{tprA}-*tprA*) x Spn037
Spn141	*rpsL1* Δ*bgaA*::(*tet* P_{phrA}-*lacZ*) Δ*amiC*(spd1670)<>*erm*	Str, Tet, Erm	E012 x Spn007
Spn165	*rpsL1* Δ*tprA* Δ*bgaA*::(*tet* P_{phrA}-*lacZ*) Δ*amiC*(spd1670)<>*erm*	Str, Tet, Erm	E012 x Spn013
Spn177	*rpsL1* CEP::(P_c-*erm rpsL*$^+$)	Str, Erm	CEP::(P_c-*erm*^{R}-*rpsL*$^+$) x IU1781
Spn182	*rpsL1* Δ*tprA* Δ*bgaA*::(*tet* P_{phrA}-*lacZ*) CEP::(P_c-*erm rpsL*$^+$)	Erm, Tet	CEP::(P_c-*erm*^{R}-*rpsL*$^+$) x Spn013
Spn184	*rpsL1* Δ*tprA* spd1717::(*kan* Tn4001*luxABCDE*) CEP::(P_c-*erm rpsL*$^+$)	Erm, Kan	CEP::(P_c-*erm*^{R}-*rpsL*$^+$) x Spn052
Spn187	*rpsL1* Δ*bgaA*::(*tet* P_{phrA}-*lacZ*) CEP::(P_{fcsK}-*phrA*Δ52-56)	Str, Tet	CEP::(P_{fcsK}-*phrA*Δ52-56) x Spn041
Spn189	*rpsL1* Δ*bgaA*::(*tet* P_{phrA}-*lacZ*) CEP::(P_{fcsK}-*phrA*Δ47-56)	Str, Tet	CEP::(P_{fcsK}-*phrA*Δ47-56) x Spn041
Spn191	*rpsL1* Δ*bgaA*::(*tet* P_{phrA}-*lacZ*) CEP::(P_{fcsK}-*phrA*Δ42-56)	Str, Tet	CEP::(P_{fcsK}-*phrA*Δ42-56) x Spn041
Spn195	*rpsL1* Δ*trpA* Δ*bgaA*::(*tet* P_{phrA}-*lacZ*) CEP::(P_{tprA}-*tprA)*	Str, Tet	Spn075 x Spn182
Spn197	*rpsL1* Δ*tprA* SPD_1717::(*kan* Tn4001*luxABCDE*) CEP::(P_{tprA}-*tprA*)	Str, Kan	Spn075 x Spn184
Spn211	*rpsL1* Δ*tprA*::(*erm rpsL*$^+$) SPD_1717::(*kan* Tn4001*luxABCDE*)	Str, Kan, Erm	Δ*tprA*::[P_c-*erm*^{R}-*rpsL*$^+$] x Spn052
Spn221	*rpsL1* Δ*tprA*::*tprA*$^+$ spd1717::(*kan* Tn4001*luxABCDE*)	Str, Kan	IU1781 x Spn211
Spn243	*rpsL1* Δ*bgaA*::(*tet* P_{phrA}-*lacZ*) CEP::(P_{fcsK}-*phrA*Δ56)	Str, Tet	CEP::(P_{fcsK}-*phrA*Δ56) x Spn041

[1]All strains are derivatives of *S. pneumoniae* D39, which is strain IU1690 in this study. *S. pneumoniae* D39 systematic gene names (where noted) are given as "SPD" followed by the gene number.
[2]Antibiotic resistance markers: Erm, erythromycin; KanR kanamycin; Str, streptomycin; Tet, tetracycline
[3]Listed are references or methods of strain construction. Strain construction is indicated as "DNA x strain transformed". An allele name indicates that this allele was newly constructed by PCR and transformed into the indicated strain. A strain number indicates that the relevant allele of this strain was PCR amplified and the resulting PCR product was transformed into the indicated strain. Primers and amplicon construction are described in Table S6 and Table S7, respectively.

Table S6. Oligos used in this study

Oligos Used in assembly of gene constructs

Name	Sequence (5' to 3')
BL1300	CCGGTAGTGGGAAAACAACTATTGGTCGTGC
BL1451	GGCTTCTTGTTCAAATTTTCCCATTTGATTCTC
BL1454	ATCATGGCGACCACACCCGTCCTGTGGATCTATCGATGCCTGAATTTCTCTGCGAGTGTATTCAT
BL1455	GTAAAACGACGGGATCAAGATGTTTCATATTTGCCTCCTTAACTAGTTAGGCGTTTTTTTCTCATGCAATGAAACC
BL1463	CCCGATATTTTGCACGAGAATGGTCGCTTTTCATTATAGGTCATATGG
BL1465	CCATATGACCTATAATGAAAAGCGACCATTCTCGTGCAAAATATCGGG
BL1466	GCAAAAGAAGTCCAATGGTCTTGATGTCGCTTTTCATTATAGGTCATATGG
BL1467	CGAGTGCAATCGCAAAAGAAGGTCGCTTTTCATTATAGGTCATATGG
BL1468	GAAGAATAAACAATTGGAGATTCGAGTGGTCGCTTTTCATTATAGGTCATATGG
BL1469	CCATATGACCTATAATGAAAAGCGACATCAAGACCATTGGACTTCTTTTGC
BL1470	CCATATGACCTATAATGAAAAGCGACCTTCTTTTGCGATTGCACTCG
BL1471	CCATATGACCTATAATGAAAAGCGACCACTCGAATCTCCAATTGTTTATTCTTC
BL1478	AAATGTAACTAATTTTTTAATTCCACGTTTTTTTCTCATTTTTCTTCTCTCTTCGTCCTTG
BL1479	CAAGGACGAAGAGAGAAGAAAAATGAGAAAAAAACGTGGAATTAAAAAATTAGTTACATTT
BL1480	GGTTTCATTGCATGAGAAAAAAACGCTCGAGCTTAGCTGACTTCAACCCA
BL1481	CGTTAAATAACCTGTAAGGCTGATAGGTCGCTTTTCATTATAGGTCATATGG
BL1482	TGGGTTGAAGTCAGCTAAGCTCGAGCGTTTTTTTCTCATGCAATGAAACC
BL1483	CCATATGACCTATAATGAAAAGCGACCTATCAGCCTTACAGGTTATTTAACG
BL1484	CTTGTTGTCTTTGCCACAACGAGTCTGAGC
BL1486	CTTAACCGAATTTGGGACAAGATAGGCTGC
BL1499	CTGTAGAAAAGAGGAAGGAAATAATAAATGAACAAAAATATAAAATATTCTCAAAACTTT
BL1500	GTTTTTTTATTTTTGGTGAATTCTAGGTACTATTATTTCCTCCCGTTAAATAATAGATAACTAT
BL1601	AAAGTTTTGAGAATATTTTATATTTTTGTTCATTTATTATTTCCTTCCTCTTTTCTACAG
BL1602	ATAGTTATCTATTATTTAACGGGAGGAAATAATAGTACCTAGAATTCACCAAAAATAAAAAAAC
BL1612	AAGAAAAGAGTTGAGACTCTCCCAACAAGGATCCGTTTGATTTTTAATGGATAATGTG
BL1613	ATTTTCTATCTTCATCAACATTAAAGGATTGTTGGGCCCCTTTCCTTATGCTTTTG
BL1614	CACATTATCCATTAAAAATCAAACGGATCCTTGTTGGGAGAGTCTCAACTCTTTTCTT
BL1615	CAAAAGCATAAGGAAAGGGGCCCAACAATCCTTTAATGTTGATGAAGATAGAAAAT
BL1630	CCATATGACCTATAATGAAAAGCGACCGCCTTCCCAACATCAAGAC
BL1631	GTCTTGATGTTGGGAAGGCGGTCGCTTTTCATTATAGGTCATATGG
erm forward	ATGAACAAAAATATAAAATATTCTCAAAACTTT
erm reverse	TTATTTCCTCCCGTTAAATAATAGATAACTAT
kanrpsL forward	TAGGATCCGTTTGATTTTTAATGGATAATG
kanrpsL reverse	GGGCCCCTTTCCTTATGCTTTTG
P019	TAGTCGCTGCTCAACTTCCTGCTT
P020	GCCGCGAATGGCTGTCAATACTTT
P021	AAAGTTTTGAGAATATTTTATATTTTTGTTCATCGTTACTAAGAAAATCGAAACCAATGA
P022	ATAGTTATCTATTATTTAACGGGAGGAAATAAGATATTTGGATGACTATTATTGACCCAC
P665	CTTGTTGTCTTTGCCACAACGAGTCTGAGC
P666	CTTAACCGAATTTGGGACAAGATAGGCTGC
P667	CATTATCCATTAAAAATCAAACGGATCCTATTGTTGGGAGAGTCTCAACTCTTTTCTT
P668	CAAAAGCATAAGGAAAGGGGCCCAACAATCCTTTAATGTTGATGAAGATAGAAAAT
P669	TTGGTAGCTTGTCTGTCTTTGTTTACAGAGTTCAA
P670	TGAACCCTCCGCAAATTTATACCATTCCGA
P671	CATTATCCATTAAAAATCAAACGGATCCTACATAAAAACACCTAGCAATGCAAATGTAA
P672	CAAAAGCATAAGGAAAGGGGCCCGAGATTCGAGTGCAATCGCAAAAG
P1402	CATTATCCATTAAAAATCAAACGGATCCTAAACAATCCTTTAATGTTGATGAAGATAGAA
TT181	GGGTTTTAATCCGCCTTCCTTTTCTCATGCAATGAAACCCCTTT
TT182	GGGGTTTCATTGCATGAGAAAAGGAAGGCGGATTAAAACCCGATA
TT183	TATCTTCATCAACATTAAAGGATTGTTTTGTTGGGAGAGTCTCAACTCTTTTCTT
TT183	TATCTTCATCAACATTAAAGGATTGTTTTGTTGGGAGAGTCTCAACTCTTTTCTT
TT184	AAAAGAGTTGAGACTCTCCCAACAAAACAATCCTTTAATGTTGATGAAGATAGAAAAT

Table S6 continued

Oligos Used in qRT-PCR

Name	Sequence (5' to 3')	gene amplified
BL1273	AGTTACATTTGCATTGCTAGGTG	*phrA*
BL1274	GCCTTCCCAACATCAAGACCATTG	
BL1273	AGTTACATTTGCATTGCTAGGTG	
BL1275	AATCCGCCTTCCCAACATCAAG	
BL1282	CATTGTCTGCTGATGAAATGAGT	spd1747 & spd1748
BL1287	GTTGTCTTTGCCACAACGAGTCTG	
BL1283	TGACCAACTTTAATTCAAACGAA	
BL1287	GTTGTCTTTGCCACAACGAGTCTG	
BL1638	GGCAAATATCGGAGTCTTGT	spd1749
BL1639	TTTCCTTGGCTGTGTGTATC	
BL1640	GTGTTCCAGAGGGAATTGTAG	
BL1641	CTTGTTTGGACGATACGATACT	
BL1642	GGAGTGCGAAATCATAACTCTA	spd1750
BL1643	CCTCCATCATCAGCATTACTT	
BL1644	CAGTTGATGGAGGCAACTTA	
BL1645	TCTCCCAATACATCTTCTCAAA	
BL1646	TGTCTTATTGCTGCCTGAAC	spd1754
BL1647	ACGATCCTGACCTGATTCTAA	
BL1648	GAAGAATTTAGACGTGCCATTT	
BL1649	GAAAGCAACTCCTATCTCTACC	
BL1280	CAGCAGTAGGGAATCTTCGGCAAT	16S rRNA
BL1281	TACGCCCAATAAATCCGGACAACG	

Table S7. Assembly of gene constructs used in this study.

Amplicons	Primer Pairs	DNA template[a]	Product[b]
amiC<>*erm*	P019 & P021	IU1690	Flanking sequence upstream of *amiC* (1.0 kb)
	erm forward & reverse	Pc-*erm* cassette[c]	*erm* open reading frame (0.7 kb)
	P020 & P022	IU1690	Flanking sequence downstream of *amiC* (1.1 kb)
	P019 & P020	Fusion PCR	Fused *amiC*<>*erm* amplicon (2.8 kb)
Δ*tprA*::(P_c-*kan*^{R}-*rpsL*$^+$)	P665 & P667	IU1781	Flanking sequence upstream of *tprA* (1.0 kb)
	kanrpsL forward & reverse	IU3116	P_c-*kan*^{R}-*rpsL*$^+$ cassette (1.3 kb)
	P666 & P668	IU1781	Flanking sequence downstream of *tprA* (1.0 kb)
	P665 & P666	Fusion PCR	Fused *ΔtprA::[*P_c-*kan*^{R}-*rpsL*$^+$*]* amplicon (3.3 kb)
Δ*tprA*::(P_c-*erm*^{R}-*rpsL*$^+$)	BL1484 & BL1614	Spn052	Flanking sequence upstream of *tprA* (1.0 kb)
	BL1612 & BL1613	Spn177	P_c-*erm*^{R}-*rpsL*$^+$ cassette (1.3 kb)
	BL1486 & BL1615	Spn052	Flanking sequence downstream of *tprA* (1.0 kb)
	BL1484 & BL1486	Fusion PCR	Fused *ΔtprA*::[P_c-*erm*^{R}-*rpsL*$^+$] amplicon (3.3 kb)
Δ*phrA*::[P_c-*kan*^{R}-*rpsL*$^+$]	P669 & P671	IU1781	Flanking sequence upstream of *phrA* (1.0 kb)
	kanrpsL forward & reverse	IU3116	P_c-*kan*^{R}-*rpsL*$^+$ cassette (1.3 kb)
	P670 & P672	IU1781	Flanking sequence downstream of *phrA* (1.0 kb)
	P669 & P670	Fusion PCR	Fused Δ*phrA*::[P_c-*kan*^{R}-*rpsL*$^+$] amplicon (3.3 kb)
Δ*tprA*::[P_c-*erm*]	P665 & P667	IU1781	Flanking sequence upstream of *tprA* (1.0 kb)
	kanrpsL forward & reverse	Pc-*erm* cassette[c]	P_c-*erm* cassette with promoter, RBS, and 3' flanking sequence of P_c-*kan*^{R}-*rpsL*$^+$ (0.9 kb)
	P666 & P668	IU1781	Flanking sequence downstream of *tprA* (1.0 kb)
	P665 & P666	Fusion PCR	Fused Δ*tprA*::[P_c-*erm*] amplicon (2.9 kb)
Δ*phrA*::[P_c-*erm*]	P669 & P671	IU1781	Flanking sequence upstream of *phrA* (1.0 kb)
	kanrpsL forward & reverse	Pc-*erm* cassette[c]	P_c-*erm* cassette with promoter, RBS, and 3' flanking sequence of P_c-*kan*^{R}-*rpsL*$^+$ (0.9 kb)
	P670 & P672	IU1781	Flanking sequence downstream of *phrA* (1.0 kb)
	P669 & P670	Fusion PCR	Fused Δ*phrA*::[P_c-*erm*] amplicon (2.9 kb)
Δ(*tprA*-*phrA*)::(*kan rpsL*$^+$)	P665 & P1402	IU1781	Flanking sequence upstream of *tprA* (1.0 kb)
	kanrpsL forward & reverse	IU3116	P_c-*kan*^{R}-*rpsL*$^+$ cassette (1.3 kb)
	P670 & P672	IU1781	Flanking sequence downstream of *phrA* (1.0 kb)
	P666 & P670	Fusion PCR	Fused Δ(*tprA*-*phrA*)::(*kan rpsL*$^+$) amplicon (3.3 kb)
unmarked Δ*tprA*	P665 & TT183	IU1781	Flanking sequence upstream of junction (0.9 kb)
	P666 & TT184	IU1781	Flanking sequence downstream of junction (1.0 kb)
	P665 & P666	Fusion PCR	Fused unmarked Δ*tprA* amplicon (1.9 kb)
unmarked Δ*phrA*	P669 & TT181	IU1781	Flanking sequence upstream of junction (0.9 kb)
	P670 & TT182	IU1781	Flanking sequence downstream of junction (0.9 kb)
	P669 & P670	Fusion PCR	Fused unmarked Δ*phrA* amplicon (1.8 kb)
unmarked Δ(*tprA*-*phrA*)	P665 & TT183	IU4955	Flanking sequence upstream of Δ*tprA* (0.8 kb)
	TT184 & P666	IU1781	Flanking sequence downstream *phrA* (1.0 kb)
	P665 & TT184	Fusion PCR	Fused unmarked Δ(*tprA*-*phrA*) amplicon (1.8 kb)
CEP::[P_{fcsK}-*phrA*]	BL1300 & BL1478	IU3131	Flanking sequence upstream of CEP::P_{fcsK} (1.5 kb)
	BL1465 & BL1479	IU1781	*phrA* open reading frame (0.2 kb)
	BL1451 & BL1463	IU3131	Flanking sequence downstream of CEP::P_{fcsK} (1.0 kb)
	BL1300 & BL1451	Fusion PCR	Fused CEP::P_{fcsK}-*phrA* amplicon (2.7 kb)
CEP::[P_{tprA}-*tprA*]	BL1300 & BL1480	IU1781	Flanking sequence upstream of CEP (0.9 kb)
	BL1482 & BL1483	IU1781	P_{tprA} and *tprA* open reading frame (1.1 kb)

	BL1451 & BL1481	IU1781	Flanking sequence downstream of CEP (1.1 kb)
	BL1300 & BL1451	Fusion PCR	Fused CEP::[P_{tprA}-*tprA*] amplicon (3.1 kb)
CEP::[P_c-*erm*^{R}-*rpsL*$^+$]	BL1300 & BL1601	IU3116	Flanking sequence upstream of CEP::[P_c-*kan*^{R}-*rpsL*$^+$] (1.0 kb)
	BL1499 & BL1500	E294	*erm* open reading frame (0.8 kb)
	BL1451 & BL1602	IU3116	Flanking sequence downstream of CEP::[P_c-*kan*^{R}-*rpsL*$^+$] (1.5 kb)
	BL1300 & BL1451	Fusion PCR	Fused CEP::[P_c-*erm*^{R}-*rpsL*$^+$] amplicon (3.3 kb)
CEP::[P_{fcsK}-*phrA*Δ52-56]	BL1300 & BL1469	Spn065	Flanking sequence upstream of CEP::[P_{fcsK}-*phrA*] (1.7 kb)
	BL1451 & BL1466	Spn065	Flanking sequence downstream of CEP::[P_{fcsK}-*phrA*] (1.0 kb)
	BL1300 & BL1451	Fusion PCR	Fused CEP::P_{fcsK}-*phrA*Δ52-56 amplicon (2.7 kb)
CEP::[P_{fcsK}-*phrA*Δ47-56]	BL1300 & BL1470	Spn065	Flanking sequence upstream of CEP::[P_{fcsK}-*phrA*] (1.7 kb)
	BL1451 & BL1467	Spn065	Flanking sequence downstream of CEP::[P_{fcsK}-*phrA*] (1.0 kb)
	BL1300 & BL1451	Fusion PCR	Fused CEP::P_{fcsK}-*phrA*Δ47-56 amplicon (2.7 kb)
CEP::[P_{fcsK}-*phrA*Δ42-56]	BL1300 & BL1471	Spn065	Flanking sequence upstream of CEP::[P_{fcsK}-*phrA*] (1.7 kb)
	BL1451 & BL1468	Spn065	Flanking sequence downstream of CEP::[P_{fcsK}-*phrA*] (1.0 kb)
	BL1300 and BL1451	Fusion PCR	Fused CEP::P_{fcsK}-*phrA*Δ42-56 amplicon (2.7 kb)
CEP::[P_{fcsK}-*phrA*Δ56]	BL1300 & BL1630	Spn065	Flanking sequence upstream of CEP::[P_{fcsK}-*phrA*] (1.7 kb)
	BL1451 & BL1631	Spn065	Flanking sequence downstream of CEP::[P_{fcsK}-*phrA*] (1.0 kb)
	BL1300 and BL1451	Fusion PCR	Fused CEP::P_{fcsK}-*phrA*Δ56 amplicon (2.7 kb)

[a] A strain number is the source of the DNA used in the PCR reaction. Fusion PCR indicates that the PCR products for an allele were combined through PCR sewing.

[b] A description of the relevant features of the PCR product is indicated with the size of the product indicated in parentheses.

[c] Pc-*erm* cassette has the same flanking 5' and 3' sequences as the Pc-[*kan*^{R}-*rpsL*$^+$] cassette. It was generated by replacing *kan*^{R}-*rpsL*$^+$ sequences with the *erm* open reading frame sequence (Tsui *et al.*, 2010).

SUPPLEMENTAL FIGURE LEGENDS

Fig S1. Structural model of a monomer of TprA.

The top panel is a three-dimensional model colored by rainbow, with the N terminus being blue and the C terminus being red. This model was generated using Phyre[2] software, and 279 residues (97% of the TprA sequence) have been modeled with 100.0% confidence by the single highest scoring template, PlcR of *B, thuringiensis*. The lower panel shows an alignment, generated by Phyre[2], between TprA of *S. pneumoniae* (the query) and PlcR of *B. thuringiensis* (the template). The green coils indicate alpha helices. Gray boxes indicate conserved residues between TprA and PlcR. The orange boxes indicate a deleted residue in TprA relative to the PlcR, and red boxes indicate a deletion in PlcR relative to TprA.

Fig S2. Deletion of *tprA* or *phrA* does not alter physiology compared to wild-type.

(A) Strains that lack either *tprA* or *phrA* show no significant difference from the parental strain with regard to growth rate, yield, or lysis during stationary phase. Strains were grown statically in BHI medium at 37°C with an atmosphere of 5% CO_2 and monitored for growth by measuring the optical density at 620 nm every hour. Starting at the entrance into stationary phase, the number of CFUs were determined every hour by serial dilution in phosphate buffered saline solution and plating on TSAII BA. The strains monitored were: black diamonds, IU1690 (D39 parental strain); gray triangles, IU4920 (D39 Δ*tprA*::*erm*); white circles, IU4922 (D39 Δ*phrA*::*erm*). Solid lines correspond to the optical density measurements; dashed lines correspond to the CFU measurements. (B) Survival curve analysis of a murine pneumonia model using intranasal inoculation of ten mice for each bacterial strain. Strains: Spn049, “wild type” parental strain used in this experiment; Spn052, Δ*tprA*; Spn053, Δ*phrA*; Spn197, Δ*tprA* CEP::TprA (complemented); Spn221, Δ*tprA*::*tprA*$^+$ (repaired). *, significant at $P < 0.05$ compared to “wild type” in log-rank (Mantel-Cox) tests. Both the complemented and repaired strains exhibited the same complete attenuation of virulence under these conditions as the *tprA* deletion strain indicating that the attenuation of virulence was not due to the lack of *tprA* but rather a background mutation that was acquired during the strain construction process.

Fig S3. qRT-PCR confirmation of induction of *phrA* expression by the 10-residue PhrA peptide.

Wild-type (IU1781) cells were grown with the 10-residue PhrA peptide or buffer alone to mid-log (OD_{620} of ~ 0.3) when RNA was isolated for qRT-PCR analysis. *phrA* mRNA amounts were normalized to 16S RNA levels and are shown as a ratio relative to the wild-type levels in buffer alone.

Fig S4. qRT-PCR confirmation of induction of *phrA* expression in CDM-galactose.

Wild-type (IU1781) cells were grown in CDM-glucose (white columns) or CDM-galactose (black columns) and RNA was isolated at the indicated time points. *phrA* mRNA amounts were normalized to 16S RNA levels and are shown as a ratio relative to the wild-type levels grown in CDM-galactose at the mid-log time point (OD_{620} of 0.3).

Fig S5. qRT-PCR confirmation of TprA/PhrA dependent regulation of select lantibiotic biosynthesis genes.

Strains: IU1781, "wild-type" parental strain used in this experiment; IU4955, Δ*tprA*; Spn075, Δ*tprA* CEP::TprA (complemented). The following conditions/strain backgrounds were compared for normalization: for analysis of the effect of synthetic peptide, IU1781 treated the 10 aa synthetic peptide was compared to IU1781 treated with the peptide resuspension buffer; for analysis of the effect of lack of TprA, IU4955 and Spn075 were compared to IU1781 (no treatments). RNA was isolated for qRT-PCR analysis from cells at mid exponential phase (OD_{620} of between 0.2 and 0.3) grown in CDM-galactose at 37°C with 5% CO_2.

Fig S6. *tprA/phrA* JBrowse snapshot.

Transcriptional patterns of the *tprA-phrA* region revealed by RNA-seq analysis. Arrangement of genes from spd1744 to 5' region of spd1749, and directions of transcription (arrows) are shown at the top track. The bottom six tracks are snapshots obtained from JBrowse genome browser (Skinner *et al.*, 2009) showing the depth of coverage of the plus (top three traces) and minus (bottom) strands obtained from RNA-seq data from WT (wild-type strain IU1781), WT + PhrA(10) (IU1781 treated with 10-residue synthetic PhrA peptide), and Δ*tprA* (Δ*tprA* strain IU4955). Different scales for the depth of coverage are shown on the right for the WT samples (maximum of 300) and the other two samples (Maximum of 6000).

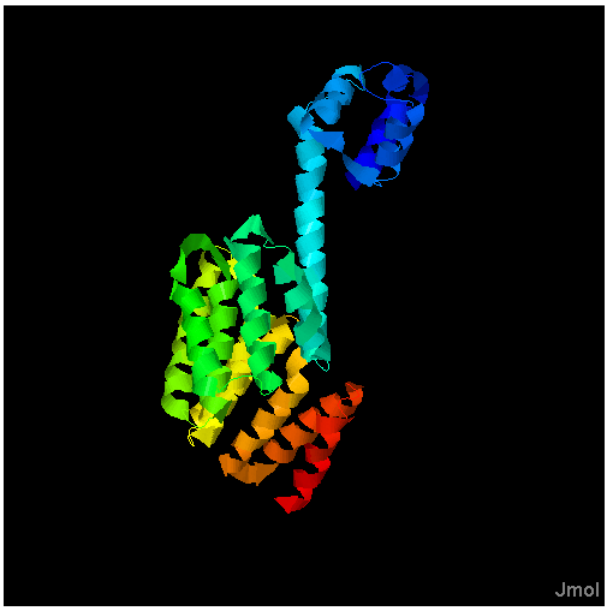
Jmol

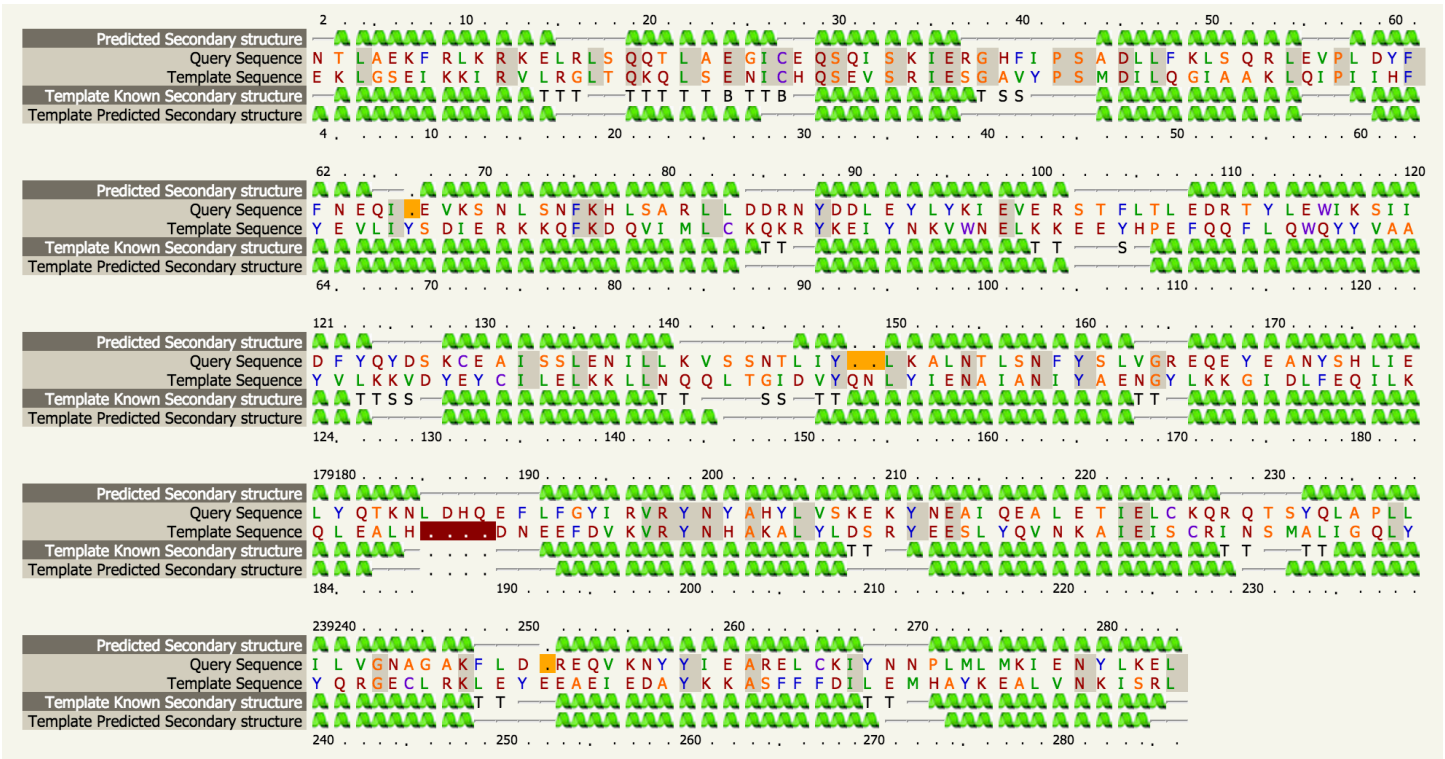
Predicted Secondary structure
Query Sequence
Template Sequence
Template Known Secondary structure
Template Predicted Secondary structure

Figure S1

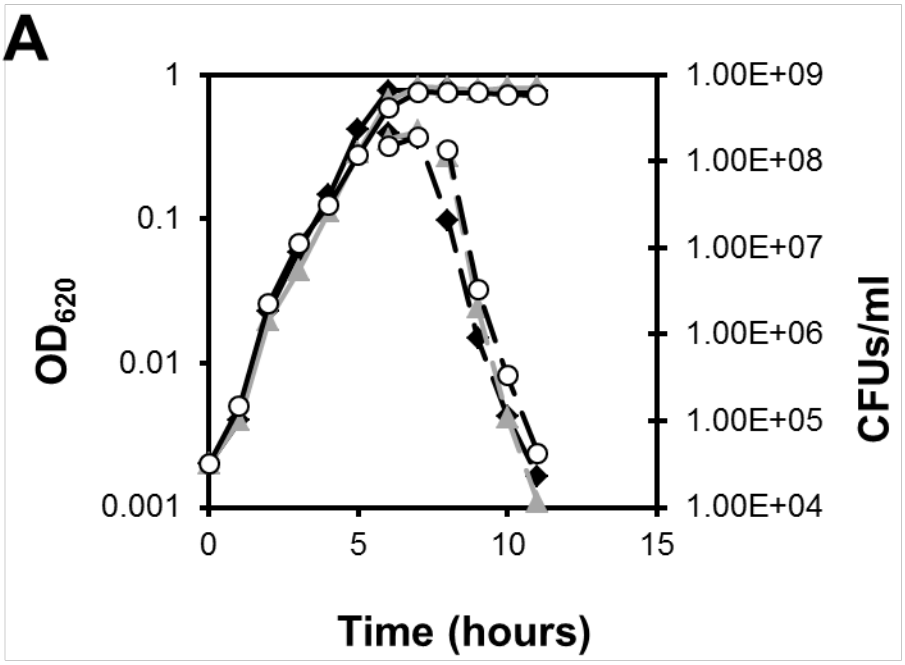
A
1
0.1
0.01
0.001
OD620
1.00E+09
1.00E+08
1.00E+07
1.00E+06
1.00E+05
1.00E+04
CFUs/ml
0
5
10
15
Time (hours)

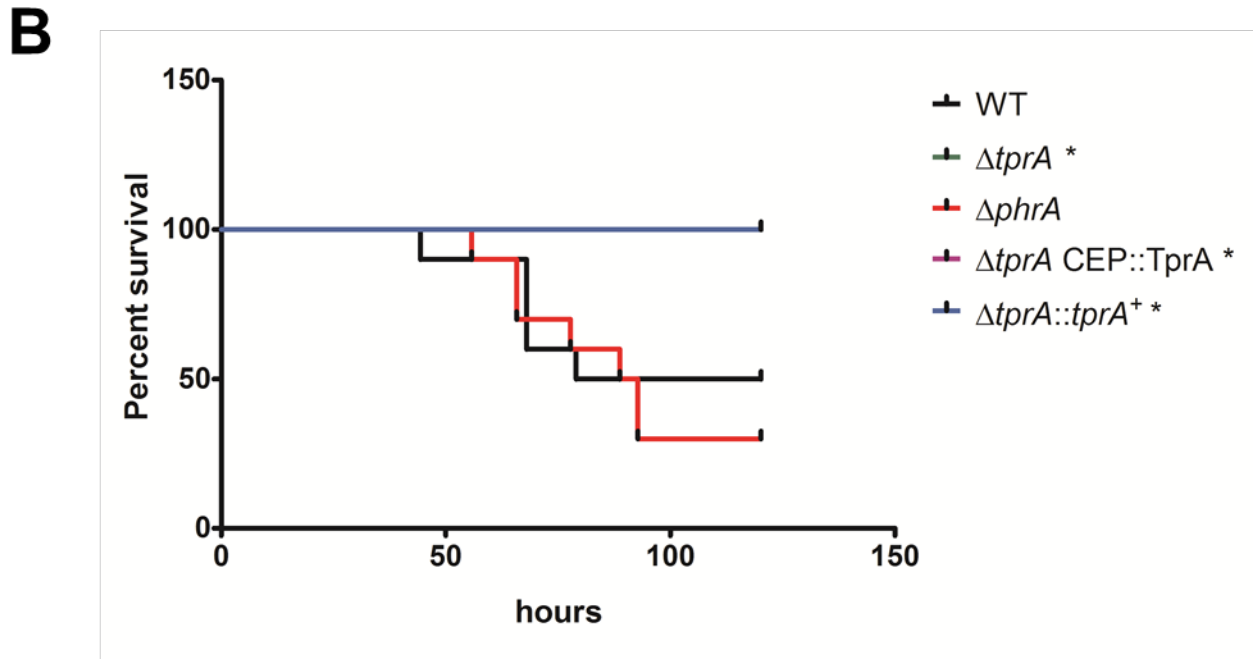
B
150
100
50
0
Percent survival
0
50
100
150
hours
WT
ΔtprA *
ΔphrA
ΔtprA CEP::TprA *
ΔtprA::tprA+ *

Figure S2

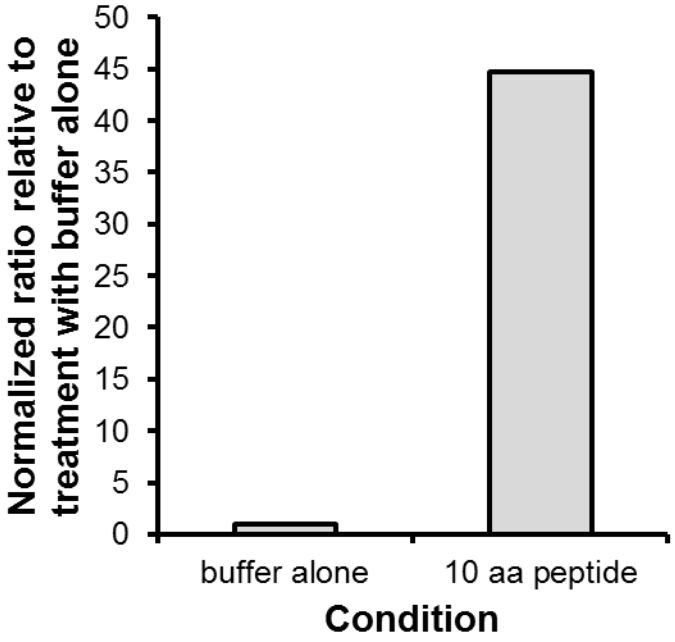
Normalized ratio relative to treatment with buffer alone
50
45
40
35
30
25
20
15
10
5
0
buffer alone
10 aa peptide
Condition

Figure S3

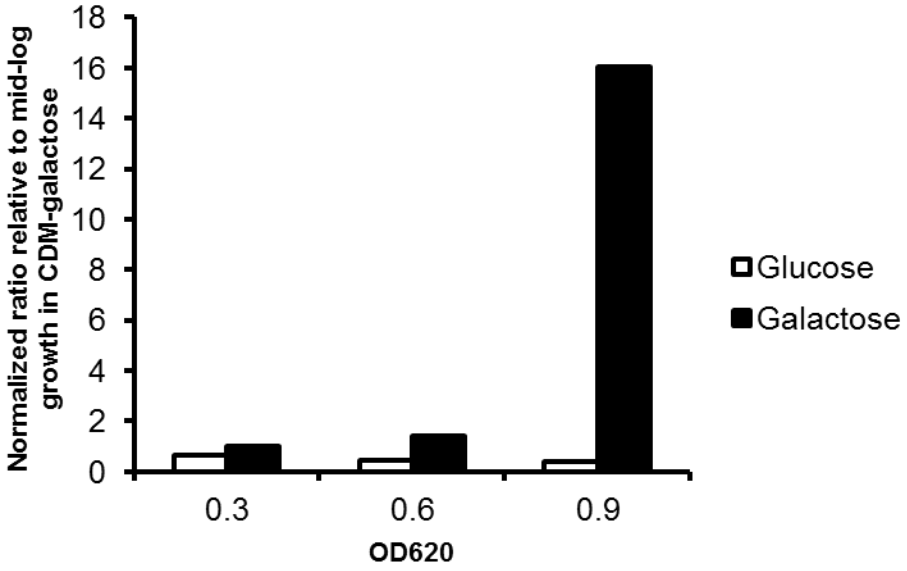
Normalized ratio relative to mid-log growth in CDM-galactose
18
16
14
12
10
8
6
4
2
0
0.3
0.6
0.9
OD620
Glucose
Galactose

Figure S4

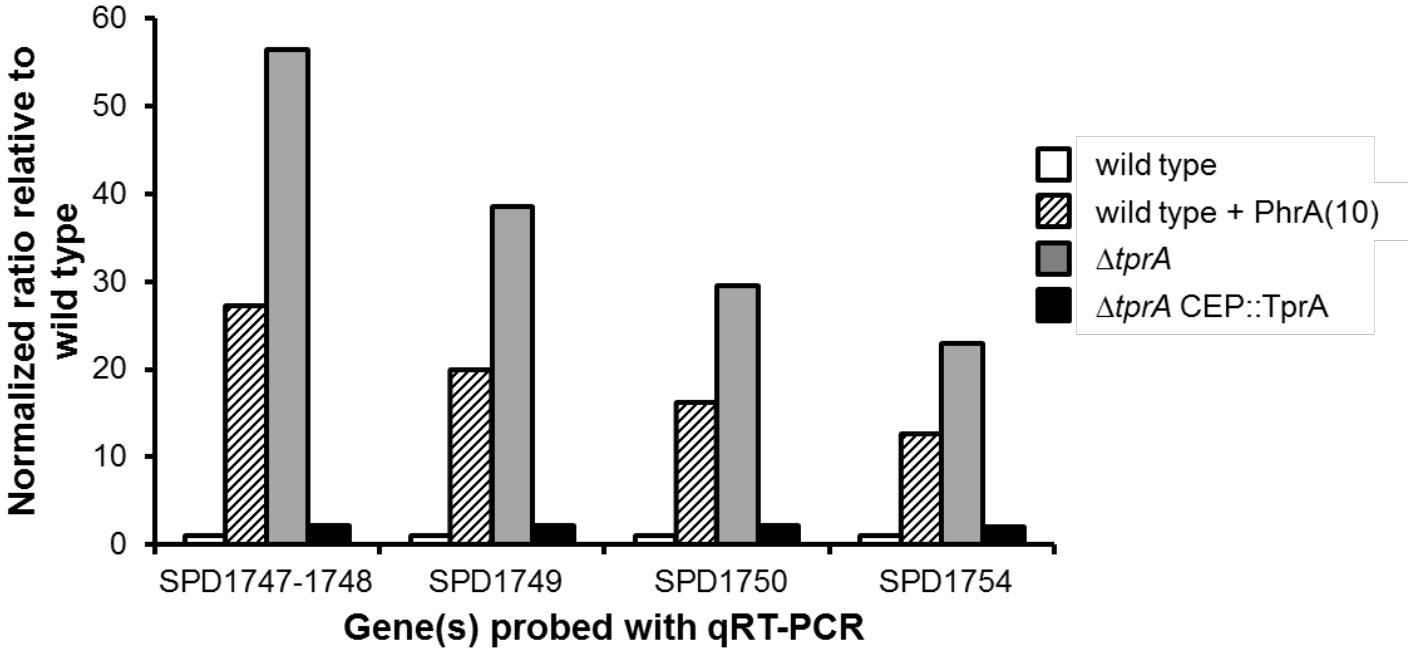
Normalized ratio relative to wild type
60
50
40
30
20
10
0
SPD1747-1748
SPD1749
SPD1750
SPD1754
Gene(s) probed with qRT-PCR
wild type
wild type + PhrA(10)
ΔtprA
ΔtprA CEP::TprA

Figure S5

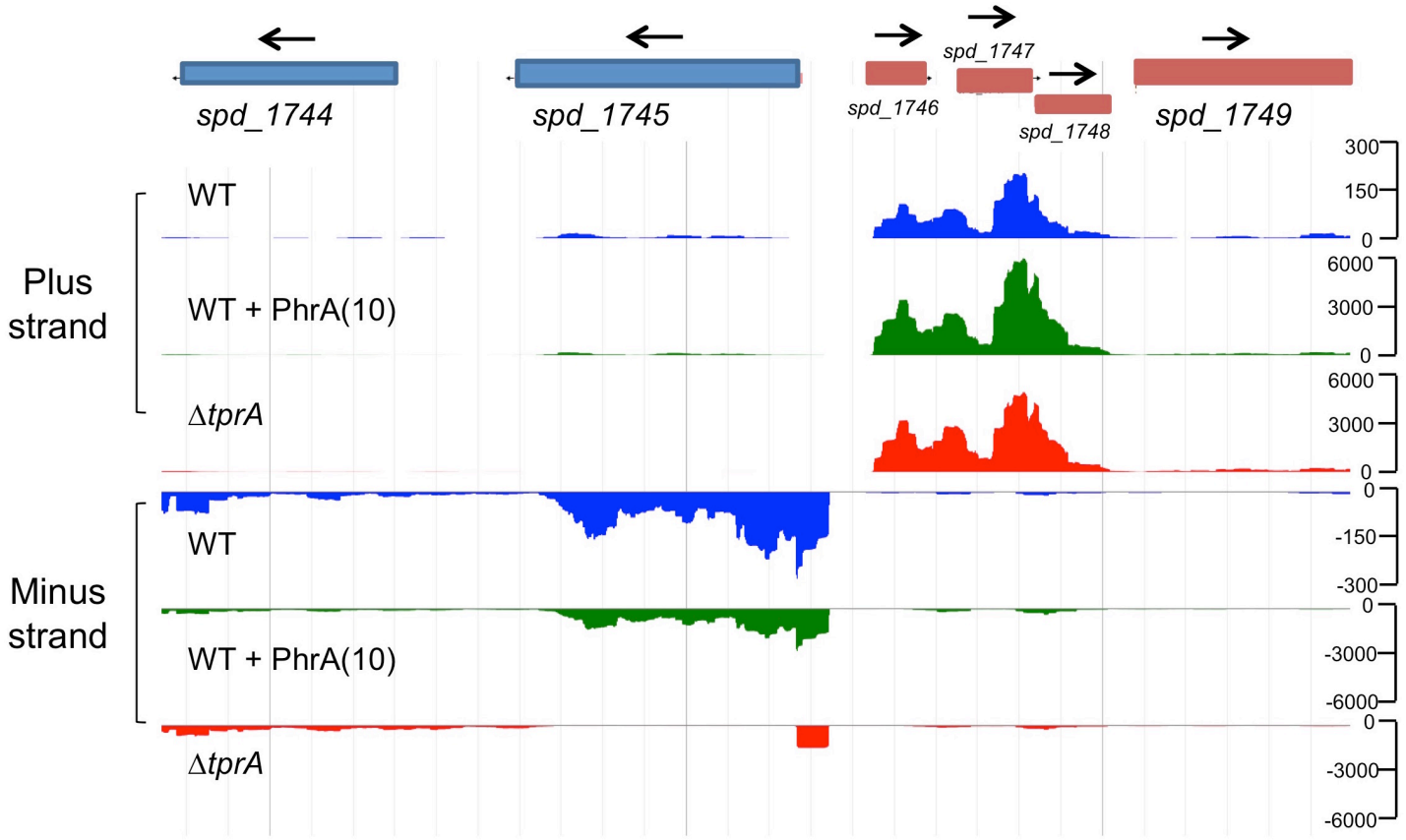
spd_1744
spd_1745
spd_1746
spd_1747
spd_1748
spd_1749
Plus strand
WT
WT + PhrA(10)
ΔtprA
Minus strand
WT
WT + PhrA(10)
ΔtprA
300
150
0
6000
3000
0
6000
3000
0
0
-150
-300
0
-3000
-6000
0
-3000
-6000

Figure S6